Article

Cell Reports

The *Galleria mellonella* Hologenome Supports Microbiota-Independent Metabolism of Long-Chain Hydrocarbon Beeswax

Graphical Abstract

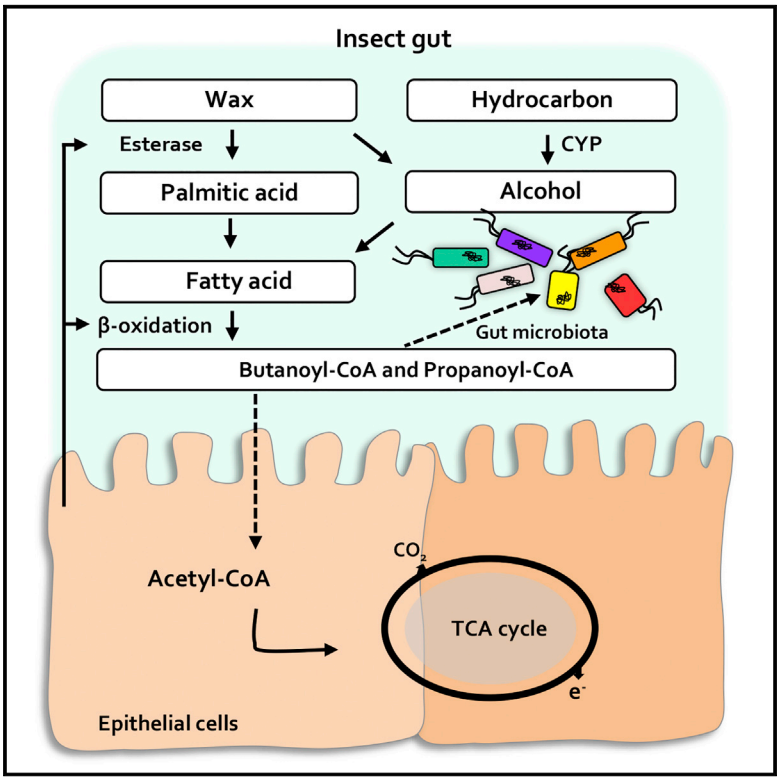

Authors

Hyun Gi Kong, Hyun Ho Kim, Joon-hui Chung, ..., Seung Gu Park, Jong Bhak, Choong-Min Ryu

Correspondence

cmryu@kribb.re.kr

In Brief

The evolutionarily expanded long-chain fatty acid degradation gene products of *Galleria mellonella* decompose long-chain hydrocarbons independently of intestinal microorganisms. Kong et al. show that beeswax and degradation products are detected equally in larvae in the presence or absence of intestinal microbes.

Highlights

- The weight of *G. mellonella* larvae is maintained by feeding wax in germ-free conditions
- Intestinal beeswax metabolism is similar regardless of intestinal microbiota
- Genome and RNA sequencing provides insights into molecular mechanisms of wax degradation
- Polyethylene metabolism can occur independently of intestinal microbiota

Kong et al., 2019, Cell Reports *26*, 2451–2464
February 26, 2019
https://doi.org/10.1016/j.celrep.2019.02.018

CellPress

Cell Reports
Article

The *Galleria mellonella* Hologenome Supports Microbiota-Independent Metabolism of Long-Chain Hydrocarbon Beeswax

Hyun Gi Kong,[1,4] Hyun Ho Kim,[3,4] Joon-hui Chung,[1,4] JeHoon Jun,[3] Soohyun Lee,[1] Hak-Min Kim,[2] Sungwon Jeon,[2] Seung Gu Park,[2] Jong Bhak,[2,3] and Choong-Min Ryu[1,5,*]
[1]Molecular Phytobacteriology Laboratory, Infection Disease Research Center, KRIBB, Daejeon 34141, South Korea
[2]Biomedical Engineering, Ulsan National Institute of Science and Technology, Ulsan 44919, South Korea
[3]The Clinomics Institute, Ulsan National Institute of Science and Technology, Ulsan 44919, South Korea
[4]These authors contributed equally
[5]Lead Contact
*Correspondence: cmryu@kribb.re.kr
https://doi.org/10.1016/j.celrep.2019.02.018

SUMMARY

The greater wax moth, *Galleria mellonella,* degrades wax and plastic molecules. Despite much interest, the genetic basis of these hallmark traits remains poorly understood. Herein, we assembled high-quality genome and transcriptome data from *G. mellonella* to investigate long-chain hydrocarbon wax metabolism strategies. Specific carboxylesterase and lipase and fatty-acid-metabolism-related enzymes in the *G. mellonella* genome are transcriptionally regulated during feeding on beeswax. Strikingly, *G. mellonella* lacking intestinal microbiota successfully decomposes long-chain fatty acids following wax metabolism, although the intestinal microbiome performs a supplementary role in short-chain fatty acid degradation. Notably, final wax derivatives were detected by gas chromatography even in the absence of gut microbiota. Our findings provide insight into wax moth adaptation and may assist in the development of unique wax-degradation strategies with a similar metabolic approach for a plastic molecule polyethylene biodegradation using organisms without intestinal microbiota.

INTRODUCTION

In recent decades, plastics have been routinely released into the environment via sewage treatment plants, waste disposal, and aerial deposition, and global plastic production has expanded tremendously worldwide (Nowack and Bucheli, 2007). Plastic disposal is one of the biggest problems facing the environment, because vast amounts of synthetic plastic remain nondegradable (Nkwachukwu et al., 2013). Plastics are synthetic polymers composed of carbon, hydrogen, oxygen, and chloride that are derived from multiple sources, such as petroleum, coal, and natural gas. The most widely used plastics polymers are polyethylene (PE), polypropylene (PP), PE terephthalate (PET), polystyrene (PS), and polyvinyl chloride (PVC) (Wu et al., 2017). PE, the most common petroleum-based plastic, is widely used in everyday life. However, the high durability and short usage time of PE is resulting in rapid accumulation in the environment, raising international interest (Ammala et al., 2011; Roy et al., 2011; Shah et al., 2008; Zettler et al., 2013).

The potential to decompose plastics in various environments has been studied in order to investigate biological degradation as a solution to accumulating plastics in the environment (Albertsson and Karlsson, 1988; Artham et al., 2009; Jones et al., 1974; Ohtake et al., 1998; Pegram and Andrady, 1989). Biodegradation of PE in the environment occurs mainly through the biological activity of microorganisms after thermal oxidation (Albertsson et al., 1987; Tokiwa et al., 2009). PE is decomposed into low-molecular-weight substances such as alkanes, alkenes, ketones, aldehydes, various alcohols, and fatty acids (Albertsson et al., 1987, 1998; Tokiwa et al., 2009). More than 90 genera of bacteria and fungi have been proposed to possess the ability to break down plastics (Mahdiyah and Mukti, 2013). However, many plastic components are recalcitrant to biodegradation by microorganisms, and the processing capacity is a generally very slow (Singh and Gupta, 2014). Metabolism of long-chain hydrocarbons is the most important step in the biodegradation of PE. This activity has not previously been reported in microorganisms. Interestingly, naturally occurring beeswax is a natural substance consisting of palmitoleate, long-chain aliphatic alcohols, and hydrocarbons. Similarly, PE is composed of a long-chain linear backbone of carbon atoms. The production of long-chain fatty acids and long-chain ethanol from beeswax is the most important process in long-chain hydrocarbon degradation. However, the associated genes and enzymes have not been studied in microorganisms.

Alternatively, the potential to metabolize long-chain hydrocarbons using insects has been studied extensively, because the enzymes and mechanisms mediating the biodegradation of long-chain hydrocarbons in environmental microorganisms remain elusive. However, *Tenebrio molitor* larvae (or mealworms) from a source in Beijing showed PS-degrading capacity, and a gut-PS-degrading *Exiguobacterium* spp. strain YT2 was isolated. The ubiquity of gut-microbiota-dependent PS degradation by mealworms was demonstrated later (Yang et al., 2018a, 2018b). Mealworms can also biodegrade PE (Brandon et al.,

2018). Using *T. molitor* from Beijing, China and other five sources from the United States, when mealworms were fed a diet containing antibiotics (gentamicin), the depolymerization of PS was inhibited, suggesting that the gut microbiota plays an important or major role in PS depolymerization. The PE-degrading strains *Enterobacter asburiae* YT1 and *Bacillus* sp. YP1 were isolated from the Indianmeal moth (*Plodia interpunctella*), which belongs to a different subfamily of the greater wax moth (*Galleria mellonella*) (Yang et al., 2014). Yang et al. found that Indianmeal moths ate PE film and isolated two PE-degraders, but they did not report evidence of depolymerization and biodegradation of PE by Indianmeal moth. Many studies have been conducted to investigate the metabolism of bacteria, especially intestinal microbiota and interactions in host organisms (El Aidy et al., 2013; Hillman et al., 2017; Hsiao et al., 2008; Rowland et al., 2018). The metabolism of long-chain hydrocarbons should be distinguished from mastication and digestion when investigating the potential for PE degradation using insects; digestion leading to an energy source can be regarded as true metabolism of PE. Analysis of nutritional mutualisms between animals and microbiota suggests that the intestinal microbiota performs an important function in food digestion (McFall-Ngai et al., 2013). A gentamicin application test was also performed with mealworms from other five sources in the United States (Yang et al., 2018b). Depolymerization of PS was inhibited, but other plastics as PE was not tested. Therefore, it is not yet known whether PE depolymerization is inhibited in the presence of gentamicin in mealworms. In *P. interpunctella*, *Bacillus* sp. YP1 and *Enterobacter asburiae* YT1 were examined for their PE biodegradation capacity (Yang et al., 2014). However, the two bacteria strains isolated from *P. interpunctella* and one strain from *T. molitor* were not tested for their ability to utilize long-chain fatty acids. Long-chain hydrocarbon metabolism is very important for the degradation of PE and beeswax (Pathak, 2017; Wilkes and Aristilde, 2017). It is difficult to understand PE metabolism without mentioning such long-chain hydrocarbon metabolism. Therefore, it should be considered whether this microorganism really plays a critical role in the PE and beeswax digestion system. Furthermore, the role of *G. mellonella*'s own enzymes and intestinal microbiota in wax degradation remains poorly understood under *in situ* and *in vitro* conditions. Microbial activity through isolation and culture does not represent all of the wax-degradation phenomena that occur in the insect gut. The decrease in PS degradation with antibiotic treatment in mealworms was confirmed, but the degradation of PE, which constitutes more of the plastic components, was not performed (Yang et al., 2018b). Therefore, a sophisticated study of PE degradation by intestinal microbiota needs be performed *in situ*. No study has been conducted to show whether *G. mellonella* without certain microbes or microbiota is capable of complete wax degradation using an energy source. Therefore, it is important to identify the role of *G. mellonella*'s own enzymes and intestinal microbiota in beeswax or PE degradation.

G. mellonella is a species of Lepidoptera that is found worldwide (Kwadha et al., 2017). The larvae of *G. mellonella* have evolved habitats and feeding strategies very different from other moths. They live on honeycomb in beehives and eat honey, beeswax, and the skin of bee pupae (Klein et al., 2007; Martel et al., 2006; Oldroyd, 1999, 2007). These foods require special behavioral and chemical strategies to allow them to be used as an energy source, such as those evolved by *G. mellonella* (Labandeira, 1997). Because beeswax is similar to PE in terms of structure, the special behavioral and chemical strategies for beeswax metabolism make *G. mellonella* a promising insect in which to investigate the potential for metabolism of PE. Beeswax is a complex material biosynthesized by bees that is composed of wax esters, fatty acids, and hydrocarbons. To date, more than 300 chemical components have been identified in pure beeswax, mainly monoesters (35%), hydrocarbons (14%), diesters (14%), triesters (3%), hydroxymonoesters (4%), hydroxy polyesters (8%), free fatty acids (1%), acidic polyesters (2%), free alcohols (1%), and various others yet to be identified (6%) (Tulloch, 1980).

Previous studies demonstrate the potential degradation of PE using isolated intestinal microorganisms. However, a complete understanding of the role of the microbiota in the intestinal tract of naturally occurring insects during their life cycle remains to be elucidated, as does the importance of host-microbiota interactions in long-chain hydrocarbon degradation (Pathak, 2017; Wilkes and Aristilde, 2017). Similarly, these results were unable to reveal the mechanisms underlying long-chain hydrocarbon hydrolysis and the genes or enzymes involved. We attempted to confirm the role of the intestinal microbiota in beeswax and PE degradation by *G. mellonella* through hologenomic analysis. In this study, we found that beeswax degradation also occurs in *G. mellonella* by eliminating intestinal microorganisms using an antibiotic cocktail treatment. Therefore, a reference genome of *G. mellonella* was constructed to identify potential enzymes encoded in the genome of the host that degrade long-chain hydrocarbons such as beeswax. Genetic analysis allowed us to identify potential *G. mellonella* enzymes that are likely to degrade long-chain hydrocarbons. In addition, transcriptional analysis of intestinal microbiota suggests that bacterial enzymes assist short-chain fatty acid degradation. Exploration of wax metabolism in *G. mellonella* at the genetic and enzymatic levels may assist the development of methods for the biological degradation of persistent PE pollutants.

RESULTS

Role of the Intestinal Microbiota in Beeswax Degradation

To determine the growth of *G. mellonella* larvae fed on beeswax, the body weight of larvae (initial size was less than 1 cm [length], and average weight was 22.9 ± 1.5 mg) fed on beeswax or nutrition-rich food, or subjected to starvation, was measured for 15 days. All larvae were maintained in starvation conditions for 3 days at the beginning of the trial to minimize the influence of previously fed food. The results showed that the weight of beeswax-fed (BW) *G. mellonella* remained constant for the entire 15-day period but increased gradually in the group fed with nutrition-rich food (NR) and decreased gradually in the starvation group (Figure 1A). In addition, weight change according to the ratio of beeswax and nutrition-rich food increased at 1:9 and 5:5 ratios compared with when nutrition-rich food alone was fed to controls (Figures 1B and 1C). These results suggest

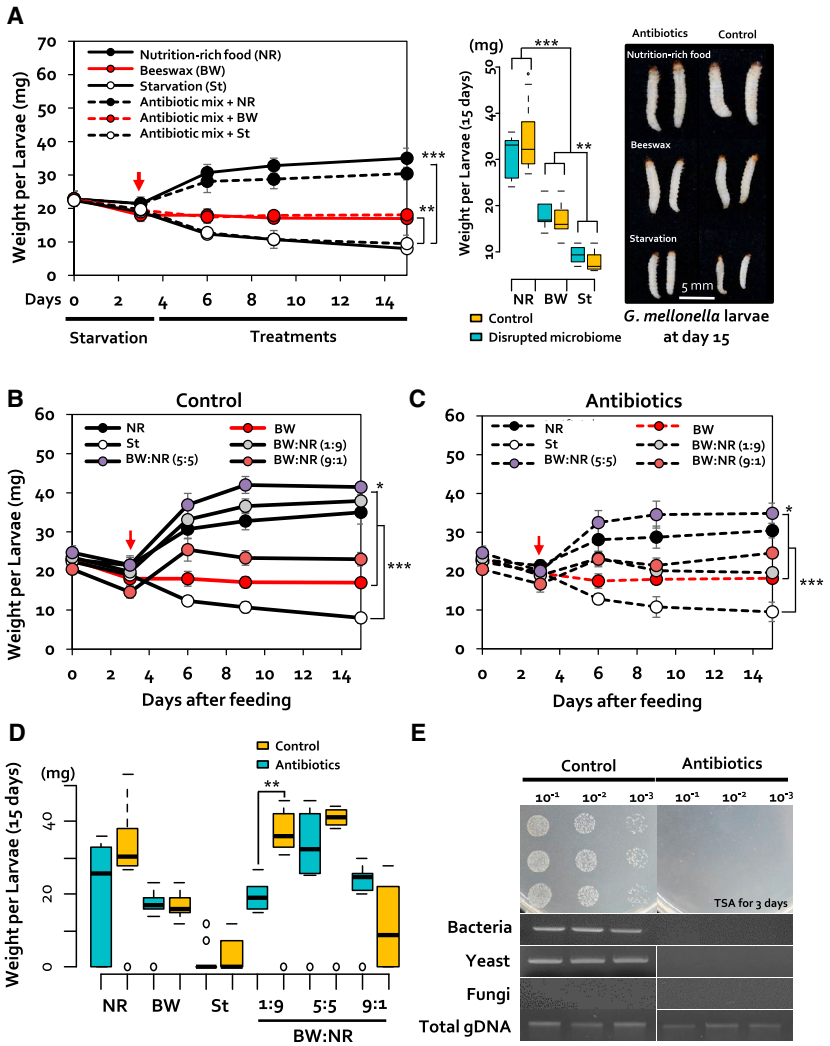

Figure 1. Weight Changes in *G. mellonella* Larvae after Wax Feeding

(A) Weight changes were investigated after feeding with beeswax or a nutrition-rich diet following 3 days of starvation. Red arrows indicate the starting point of the feeding process. Data represent mean ± SEM (n = 10, larvae).

(B and C) Weight change according to feeding in the control group (treated with PBS) (B) and intestinal microbial removal group (antibiotic treatment) (C) for 15 days. Antibiotics were used to individually treat larvae using force-feeding. Food processing was treated with 100 mg per larva, in beeswax, nutrition-rich food and mixture of 1:9, 5:5, and 9:1 ratios, respectively. Data show the mean ± SEM (n = 10, larvae).

(D) A boxplot diagram showing larval weight by feeding type. Data show the mean ± SEM (n = 10, larvae); ***p = 0.001, **p = 0.01, *p = 0.05 (two-way ANOVA followed by Tukey's honestly significant difference test).

(E) Antibiotic treatment of the intestinal microbiota using a culture or nonculture method. For the culture method, after 1 day of antibiotic treatment, intestines were removed and diluted in tryptic soy agar (TSA) media. For the uncultured method, we performed PCR using bacteria-, yeast-, and fungi-specific primers.

that feeding on beeswax can produce energy sufficient for survival.

Furthermore, we evaluated whether wax was decomposed by *G. mellonella* larvae lacking intestinal microbiota following exposure to a five-antibiotic cocktail (ampicillin for gram-negative bacteria, kanamycin for both gram-positive and gram-negative bacteria, neomycin for yeast, vancomycin for gram-positive bacteria, and polymyxin B for gram-negative bacteria) (Figure 1C). At 1 day after antibiotic treatment, the intestinal microbiota was no longer detected by culture-dependent and culture-independent methods (Figure 1E).

To investigate the role of the intestinal microbiota in wax degradation, intestinal microbiota was removed by feeding antibiotics to second-instar larvae, and growth was compared for *G. mellonella* groups with and without an intact intestinal microbiota. Interestingly, regardless of the intestinal microbiota, body weight remained constant in beeswax-fed groups and gradually increased in nutrition-rich food groups, and both body weights gradually decreased during starvation (Figure 1C). On the other hand, in the case of nutrition-rich food, the body weight of the antibiotic treatment group (mean, 30 mg) was decreased compared with that of the untreated larvae (mean, 35 mg), indicating that the microbiota plays a role in the degradation of nutrition-rich food (Figures 1A and 1B). Body weight reduction by antibiotic treatment was observed in all treatments except wax treatment and starvation treatment (Figure 1B and C). To further confirm the energy conversion of the beeswax, beeswax and nutrition-rich food were mixed with each other at ratio 1:9, 5:5 and 9:1. As a result, beeswax and nutrition-rich food (5: 5 ratio) indicated higher weight than nutrition-rich food alone regardless of intestinal microbiota (Figures 1B and 1C). Compared with antibiotic treatment and control after 15 days of feeding, we found that the weight gain of NR diet was decreased more than that of control. (Figure 1D). Therefore, beeswax can be used as an energy source for *G. mellonella* larvae. In addition, unlike beeswax, the intestinal microbiota may play a role in the digestion of nutrition-rich food.

After feeding nutrition-rich food and beeswax, we could confirm that different phenotypes appeared in the intestine and frass. This confirms that *G. mellonella* normally feeds on beeswax (Figure 2A). Beeswax is composed of esters that combine long-chain fatty acids with long-chain alcohols. Degradation of beeswax by heat treatment was investigated using gas chromatography-mass spectrometry (GC-MS), and palmitic acid was confirmed as the most abundant component identified (Regert et al., 2001). Therefore, the proportion of long-chain fatty acids can be used as a measure of the degradation of beeswax. To investigate the formation of intermediates of wax metabolism,

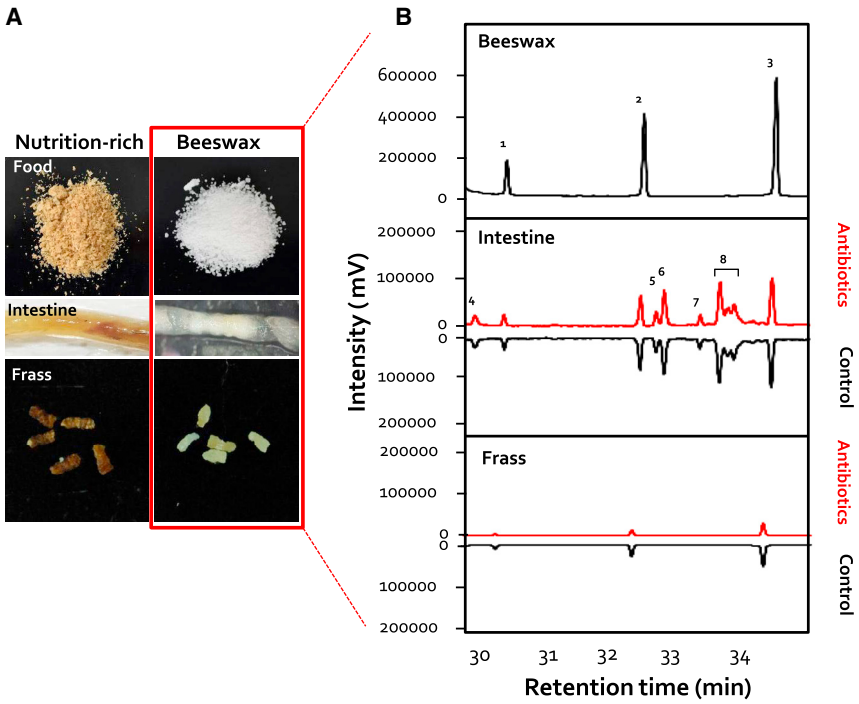

Figure 2. Role of the *G. mellonella* Intestinal Microbiota in Beeswax Degradation

Insects with (treated with PBS) and without (treated with antibiotics) intestinal microbiota displayed identical intestinal component profiles with all diets.

(A) Peak identities are as follows: 1, eicosane; 2, heptadecane; 3, tetracosane; 4, 1-heptadecanamine; 5, 5-pyrrolidine, 1-(1-oxo-7,10-hexadecadienyl)-; 6, 2-pyrrolidinone, 1-(9-octadecenyl)-; 7, Palmidrol; 8, 9-octadecenamide, (Z)-.

(B) Difference between nutrition-rich and beeswax feeding intestines and frass of *G. mellonella* larvae.

including hydrocarbons and fatty acids, in the beeswax, midgut, and frass of *G. mellonella* larvae, long-chain fatty acids were profiled by GC-MS under beeswax-fed conditions.

Long-chain hydrocarbons such as eicosane, heptadecane, and tetracosane were found in beeswax (Figure 2B). In beeswax fed with intestinal microbiota, pyrrolidine, palmidrol, and 9-octadecenamide were generated as long-chain fatty acids (Figure 2B). In addition, these metabolites and long-chain hydrocarbons were not detected in frass (Figure 2B). Interestingly, the content of these three fatty acids was largely unaffected in *G. mellonella* larvae lacking intestinal microbiota, indicating that beeswax was metabolized independently of the intestinal microbiota (Figure 2).

G. mellonella Genome Assembly and Annotation

In the GC-MS analysis, the intestinal microbiota was not important in the production of long-chain fatty acids from the metabolism of long-chain hydrocarbon wax. Therefore, we further investigated the mechanism of wax biodegradation by assessing the host *G. mellonella* genome without intestinal microbiota. A *G. mellonella* reference genome was constructed using PacBio RS II (Table S1), resulting in 32.5 Gb of data, with 65-fold coverage of the estimated 500-Mb genome with a contig number of 624 and an N50 value of the final contig of 2.8 Mb (Table S1). Sequencing data were assembled using Falcon assembler, and the final contig size was 482 Mb (Table S1). PacBio sequencing error correction was performed by replacing homo variants with 36-Gb Illumina HiSeq short read data. The assembled *G. mellonella* genome is the highest quality among Lepidoptera genomes, with >98% of *de novo* assembled transcripts (83,730 out of 85,530) successfully mapped to the assembly (Table S2). A total of 15,607 protein-coding genes were predicted using transcriptome-based gene prediction and *de novo* gene prediction, as well as homology gene prediction (Table S2). The predicted gene quality was evaluated by the BUSCO program, and 88.3% of proteins were analyzed, which is relatively high among Lepidoptera genomes (Table S3). Of the protein-coding genes, 93.64% have a homolog in publically available protein databases and were classified into functional categories according to InterPro, the Kyoto Encyclopedia of Genes and Genomes (KEGG) pathway, and Gene Ontology (GO) databases.

Evolution of Gene Families Related to Wax Degradation

To confirm the presence of gene families related to the production of long-chain fatty acids via beeswax degradation in *G. mellonella* that are absent in other moths, we performed an orthologous gene comparison using 13 insects, including *G. mellonella, Amyelios transitella, Bombyx mori, Papilio xuthus, Plutella xylostella,* and *Tetranych usurticae* as an outgroup (Figure 3A; Table S1). We identified 13,151 orthologous gene families and 7,267 gene families in *G. mellonella* that were common to all five Lepidoptera species (Figure 3B) and 2,687 specific gene families in *G. mellonella* and 1,274–3,211 species-specific gene families for other Lepidoptera species (Figure 3B). *G.-mellonella*-specific genes mainly belonged to sensory perception and peptidase-related gene families based on GO categories and the KEGG pathway (Table S4). In addition, 340 and 333 gene families were significantly expanded and contracted, respectively, in *G. mellonella* compared with the common ancestor of *G. mellonella* and *A. transitella* (Figure 3A; Table S5). Among the 340 expanded gene families, hydrolase activity, biosynthesis of unsaturated fatty acids, and cytochrome P450 (CYP) were over-represented in *G. mellonella.* Specifically, peroxisome-proliferator-activated receptor (PPAR) signaling and fatty acid metabolism and biosynthesis pathways were particularly enriched and highly expressed (Tables S5 and S13). Enrichment of the hydrolase and fatty-acid-metabolism-related gene families is indicative of the degradation of long-chain hydrocarbon wax in *G. mellonella* and the potential use of long-chain fatty acids produced from wax.

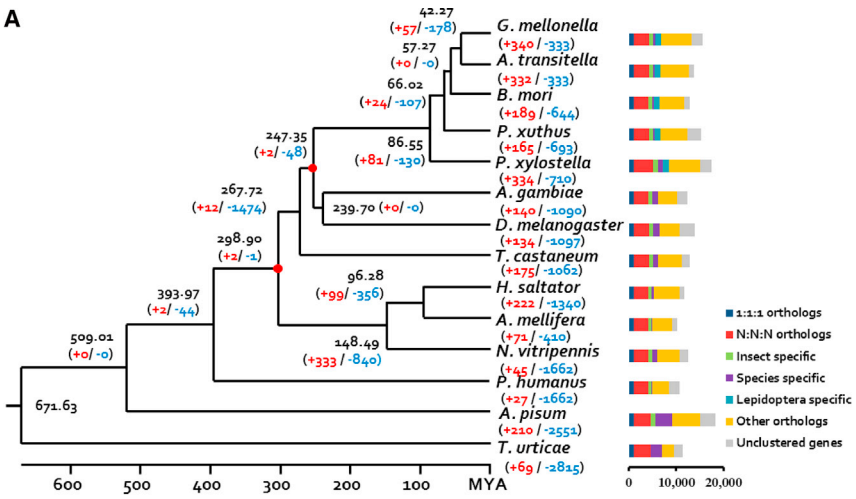

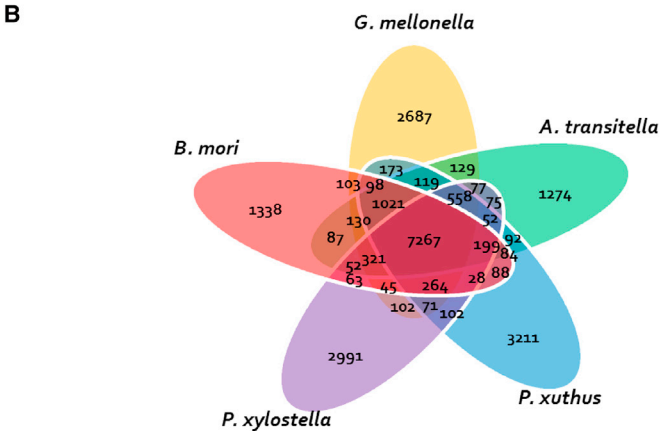

Figure 3. Phylogenetic Relationships and Genomic Comparison of *G. mellonella* with Other Lepidoptera Species

(A) Phylogenetic tree of related species. Red dots (for calibration) represent the divergence time (239.7 million years ago and 298.9 million years ago). Branch numbers represent the divergence time (black) and the number of genes expanded (red) or contracted (blue) after being separated from the last common ancestor. 1:1:1 orthologs contain a single copy of genes present in related species. N:N:N orthologs contain multiple copies of genes present in related species. Insect features appear only in insects, and other orthologs include genes that cannot be clustered.

(B) Venn diagram of shared and specific orthologous gene clusters in *G. mellonella* constructed using five insect genomes.

A total of 127 positive selection genes were calculated using 1,024 single-copy genes from 14 closely related insect species (Table S6). Interestingly, *ZDHC2* and *ZDHC6*, genes related to fatty acid oxidation, indicated positive selection in *G. mellonella*. ZDHC2 and ZDHC6 are palmitoyltransferases (Table S6) that are responsible for delivering long-chain fatty acids from the cytoplasm into mitochondria for oxidation (Qu et al., 2016).

To investigate the expression of genes related to the degradation of beeswax, changes in gene expression in the fat body and gut of *G. mellonella* were confirmed by metatranscriptome analysis after feeding with a 1:9 ratio of nutrition-rich food and beeswax or nutrition-rich food without beeswax for 12 h. The 1:9 ratio of nutrition-rich food and beeswax treatments are expected to be activated enzymes and genes involved in beeswax degradation because they exhibit weight gain in larvae compared to beeswax alone. The resulting metatranscriptome data were annotated based on the established *G. mellonella* reference genome (Table S7), and 3,255 differentially expressed genes (DEGs) were identified between beeswax-fed and beeswax-free *G. mellonella* fat body tissue (false discovery rate [FDR] < 0.05). Among the DEGs, gene families related to oxidoreductase activity and oxidation-reduction processes were enriched in the group fed with nutrition-rich food and beeswax based on GO enrichment and KEGG pathway analysis (Table S8). Hydrocarbon metabolism and fatty-acid-related pathways were especially enriched in beeswax-fed *G. mellonella* fat body tissue (Table S8). In *G. mellonella* gut samples, 1,476 genes were upregulated following feeding with beeswax, and genes related to carboxylic acid and methane metabolism were especially enriched in this group (Table S9).

Long-Chain Fatty Acid Metabolism in *G. mellonella* Responding to Beeswax

GO enrichment analysis confirmed that hydrolase activity was expanded in *G. mellonella* compared with its ancestors (Table S5). Hydrolases such as esterase and lipase catalyze chemical reactions that produce long-chain alcohols and long-chain carboxylates using wax and H_2O as substrates (Huang et al., 1978; Figure 4A). Therefore, we attempted to identify genes that might be directly responsible for long-chain hydrocarbon wax metabolism by searching for signs of selection and convergence in genes associated with hydrolase, long-chain fatty acid oxidation, and long-chain alcohol oxidation using InterProScan (Table S10). Notably, carboxylesterase and lipase 1 and 3 families were over-represented in *G. mellonella* compared with other Lepidoptera species (Figure 4B; Table S10). Moreover, transcriptome analysis revealed that carboxylesterase and lipase 1 and 3 family-related genes were overexpressed in the fed fat body and gut of groups fed nutrition-rich food with beeswax (Figure 4C). Long-chain fatty acids are intermediates generated by wax esterification that are subsequently decomposed into short-chain fatty acids via beta oxidation carried out by acetyl-coenzyme A (acyl-CoA) dehydrogenase, enoyl-CoA hydrolase, 3-hydroxyacyl-CoA dehydrogenase,

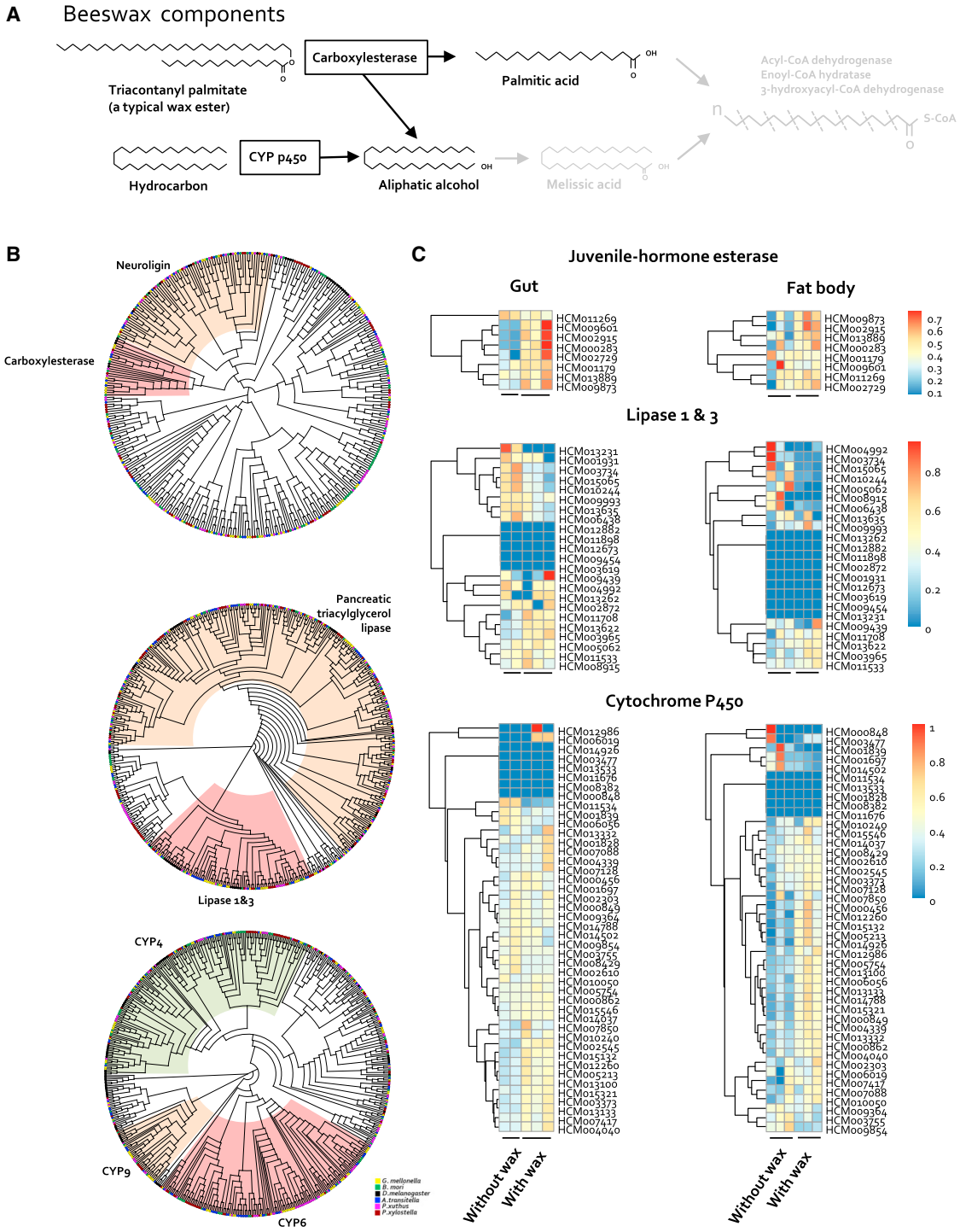

Figure 4. Expansion of Genes in *G. mellonella* and Expression Profiling of Genes Related to Long-Chain Hydrocarbon Wax Degradation following Feeding on Beeswax

(A) Schematic diagram showing the long-chain hydrocarbon wax metabolism model of *G. mellonella* that includes long-chain fatty acid metabolism branches.

(B) Phylogenetic tree of all esterase, lipase, and cytochrome P450 (CYP) enzymes present in Lepidoptera species. Light-yellow gradation represents neuroligin and acetylcholinesterase. Red gradation indicates clusters of carboxyl esterase, lipase 1 and 3, and CYP enzyme.

(C) Expression heatmap of carboxylesterase, lipase 1 and 3, and cytochrome, which is expanded in the *G. mellonella* genome. Gene expression of esterase, lipase, and cytochrome is indicated by two individual larvae for "Without wax" (duplicate) and three individual larvae for "With wax" (triplicate). In the fat body, gene expression is indicated by three individual larvae for all treatments.

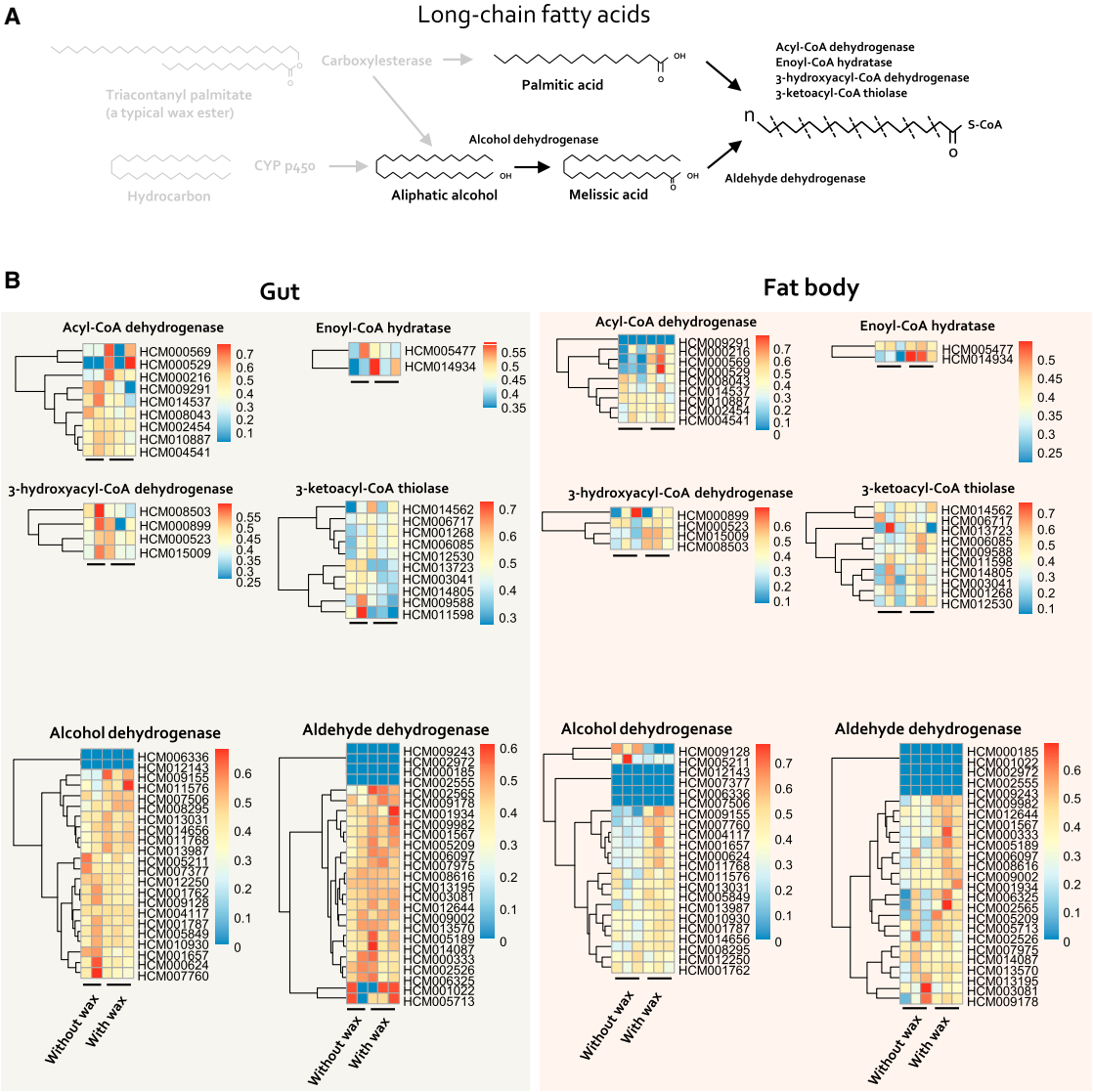

Figure 5. Expression Profiling of Genes Related to Long-Chain Fatty Acid Degradation and Long-Chain Ethanol Degradation

(A) Schematic diagram showing the wax metabolism model of *G. mellonella* that includes short-chain fatty acid metabolism branches.

(B) Expression heatmap of genes related to beta-oxidation such as acyl-CoA dehydrogenase, enoyl-CoA hydratase, 3-hydroxyacyl-CoA dehydrogenase, 3-ketoacyl-CoA thiolase, alcohol dehydrogenase, and aldehyde dehydrogenase, which are expanded in the *G. mellonella* genome. Gene expression is indicated by three individual larvae for all treatments (triplicate).

and 3-ketoacyl-CoA thiolase (Figure 5A). The *ACOX1* gene encoding acyl-CoA dehydrogenase is expanded in *G. mellonella* compared with other Lepidoptera species (Table S10), and *ACOX1* is highly activated during the processing of very-long-chain acyl-CoA (Ferdinandusse et al., 2007; Oaxaca-Castillo et al., 2007).

Analysis of Short-Chain Fatty Acid Metabolism in the Microbial Transcriptome

PE degraders were isolated from larvae of *P. interpunctella* (Lepidoptera: Pyralidae; i.e., Indianmeal moth) (Yang et al., 2014). It is also unknown whether *P. interpunctella* larvae feed on beeswax, and they could degrade PE independently of the gut microbiota. In this study, we investigated the role of the gut microbiota of *G. mellonella* in the degradation of long-chain hydrocarbon wax by transcriptome analysis of larvae fed with and without beeswax, and identified 17,514 DEGs (FDR < 0.05). Specific gene families related to short-chain fatty acids and carbon, methane, and propanoate metabolism were upregulated in intestinal microbiota form *G. mellonella* fed with beeswax, based on KEGG analysis of 802 microbiome protein sequences (Table S11). However, gene families related to the formation of long-chain fatty acids from beeswax were not overexpressed in the intestinal microbiota. Among the DEGs, the expression of lipases and cytochromes potentially related to wax degradation was decreased in intestinal microbiota fed on beeswax.

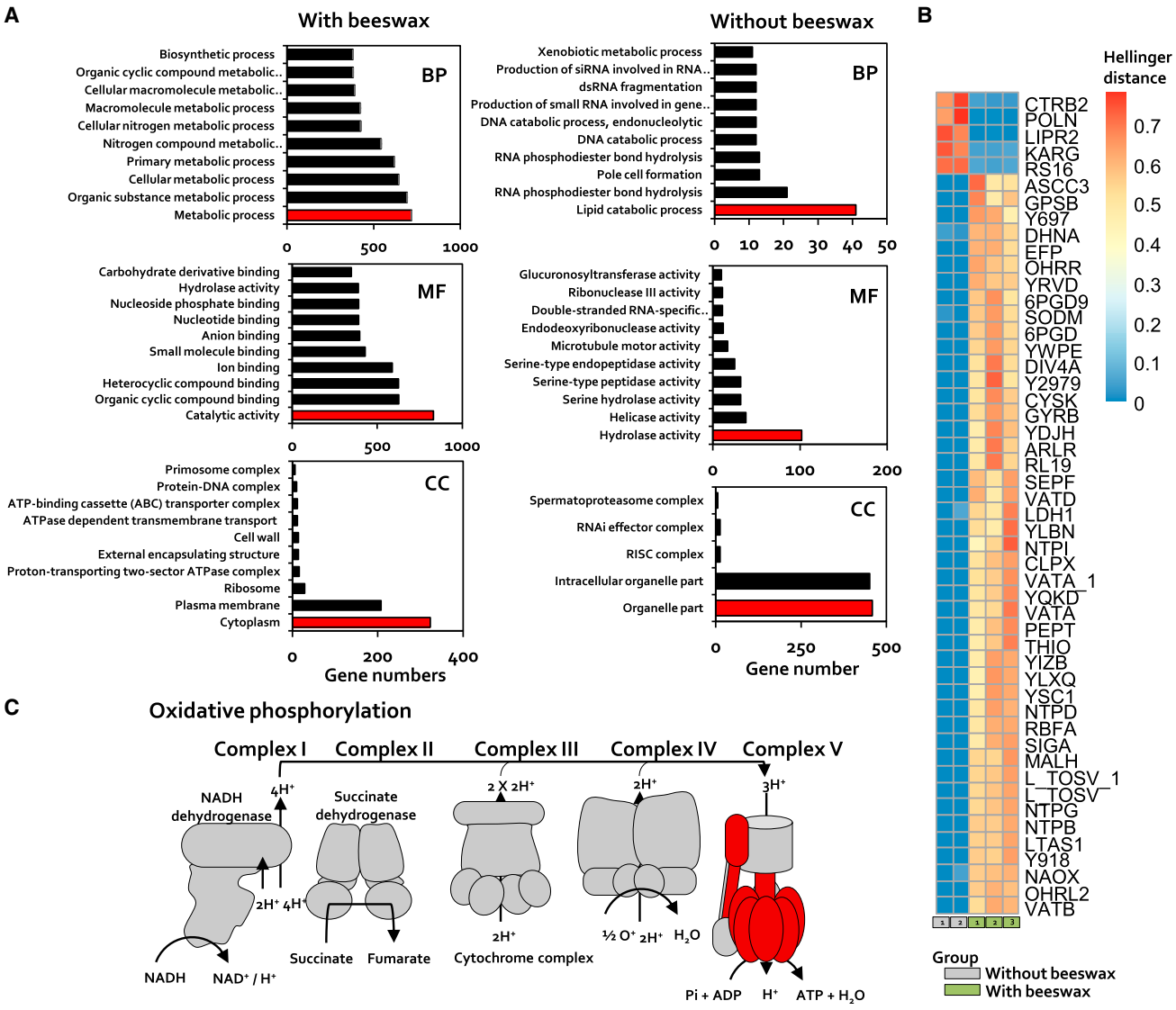

Figure 6. Profiling of Differentially Expressed Genes and Gene Ontology Clustering in the *G. mellonella* Gut Microbiome following Feeding on Beeswax

(A) Gene Ontology term classification of wax-fed and nutrition-rich diet-fed intestinal microbiota.

(B) Heatmap generated from 50 genes with the smallest false discovery rate (FDR) is shown.

(C) Oxidative phosphorylation of intestinal microbiota. Significant changes in the intestinal bacteria transcriptomic pattern between wax-fed and nutrition-rich diet-fed are indicated. Enriched transcripts are given in red.

GO enrichment analysis of DEGs revealed that metabolic process (biological process), catalytic activity (molecular function), and cytoplasm (cellular component) categories were mainly enriched in intestinal microbiota in beeswax-fed *G. mellonella* (Figure 6A). Pathways associated with the metabolism and biosynthesis of secondary metabolites were especially enriched following feeding on beeswax based on KEGG pathway analysis (Table S11). Contrary to the *G. mellonella* gut expression profile, gene families related to fat digestion and absorption, PPAR signaling, and metabolic pathways were upregulated in intestinal microbiota fed without beeswax (Table S12). We identified the most differentially expressed 50 genes with the smallest FDR, and these are shown in Figure 6B. Among those most highly affected were pathways associated with the V-type sodium ATPase subunit (e.g., NTPB, NTPD, NTPG, and NTPI), the V-type proton ATPase catalytic subunit (VATA, VATB, and VATD), and the oxidative stress response (SODM, OHRL2, and OHRR) (Figure 6C). These results suggest that metabolic mechanisms in the intestinal microbiota are altered in the presence of beeswax, especially those related to the biosynthesis of secondary metabolites, whereas those related to the production of long-chain fatty acids and long-chain ethanol from long-chain hydrocarbon wax are not affected. This result indicates that *G. mellonella* intestinal microbiota do not degrade long-chain

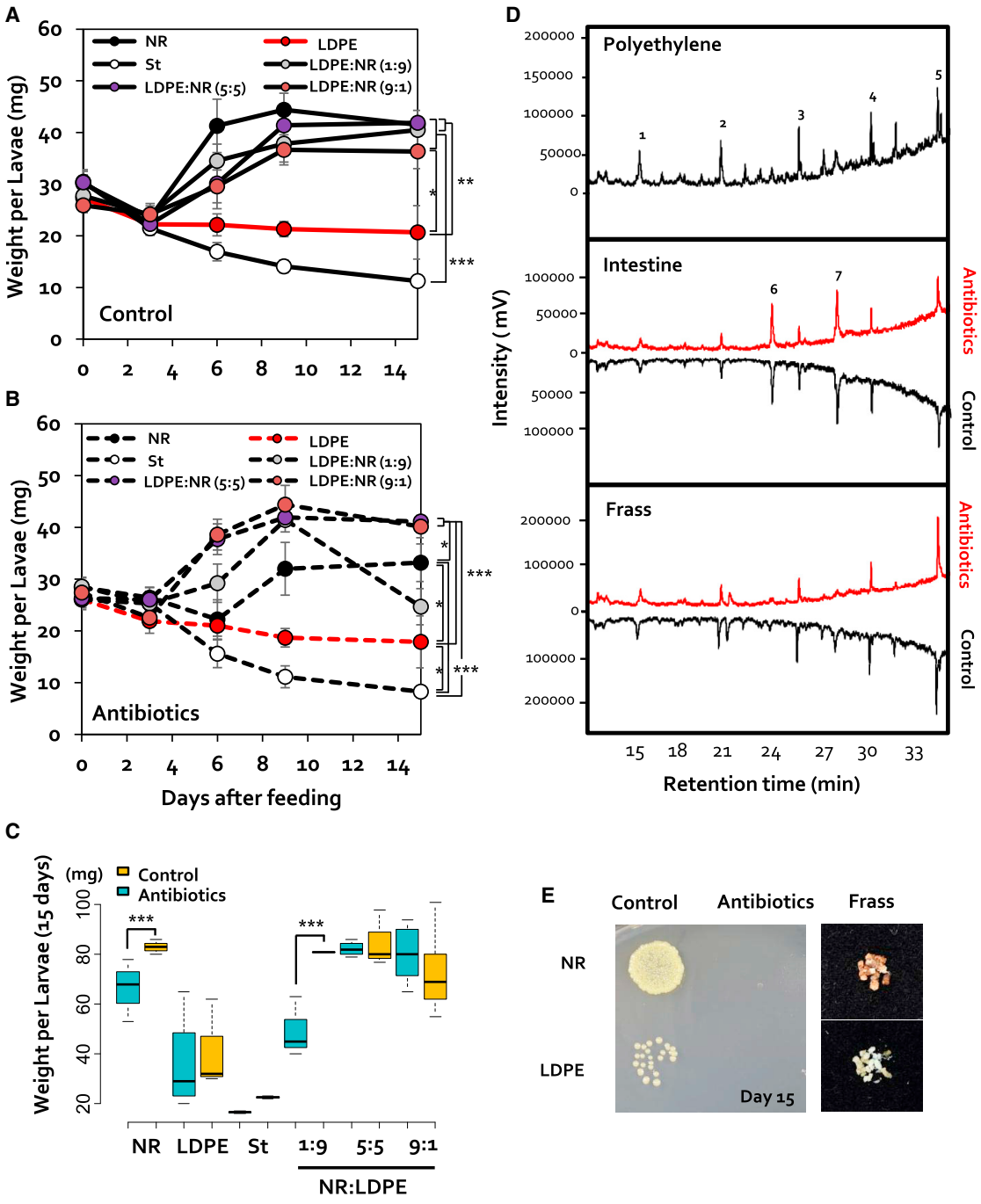

Figure 7. Weight Changes in *G. mellonella* Larvae after Polyethylene Feeding

Weight change was investigated after feeding with polyethylene or a nutrition-rich diet following 3 days of starvation. Red arrows indicate the starting point of the feeding process.

(A and B) Weight change according to feeding in the control group (treated with PBS) (A) and the intestinal microbial removal group (antibiotic treatment) (B) for 15 days. Larvae were individually treated with antibiotics using force-feeding. Food processing was treated with 100 mg per larva in polyethylene, nutrition-rich food alone and mixture of 1:9, 5:5, and 9:1 ratios, respectively. Data show the mean ± SEM (n = 10, larvae).

(C) A boxplot diagram showing larval weight by feeding type. Data show the mean ± SEM (n = 10, larvae); ***p = 0.001, **p = 0.01, *p = 0.05 (two-way ANOVA followed by Tukey's honestly significant difference test).

(legend continued on next page)

hydrocarbon wax but appear to decompose short-chain fatty acid wax degradation products. However, the role of intestinal microorganisms in the degradation of short-chain fatty acids needs to be confirmed experimentally.

Role of the Intestinal Microbiota in PE Degradation

G. mellonella was found to break down beeswax independently of the intestinal microbiota in the present study. Therefore, the degradation of PE, which is similar to the chemical structure of beeswax and causes environmental problems, was investigated through *G. mellonella* body weight changes. To determine the growth of the PE-fed *G. mellonella* larvae, the body weight of the second larva (less than 1 cm) fed either PE powder (catalog number B1180, LDPE, 500 μm, Thermo-Fisher Scientific) or nutrition-rich food or starvation was measured for 15 days (Figure S1). All larvae were kept in starvation conditions for 3 days in the beginning of the trial to minimize the effects of previously fed food. As a result, the weight of PE-treated *G. mellonella* remained constant for 15 days but gradually increased in the group fed a nutrition-rich diet and gradually decreased in the starvation group (Figures 7A and 7B). To further confirm the energy conversion of PE, PE and nutrition-rich food were mixed at ratios of 1:9, 5:5, and 9:1. The mixture of PE and nutrition-rich food was similar to that of nutrition-rich food regardless of the intestinal microbiota (Figures 7A and 7B). This suggests that PE feeding can produce enough energy for survival. In the case of 1:9 PE and nutrition-rich food, the weight decreased on the 15th day (Figure 7B). Further study is necessary to determine the cause of the sudden change in weight at the 1:9 ratio (Figures 7B and 7C).

To study the role of the intestinal microbiota in the degradation of PE, the intestinal microbiota was removed by feeding an antibiotic cocktail to second-instar larvae. Interestingly, irrespective of the intestinal microbiota, the weight of the PE-fed group remained constant, the weight of the nutrition-rich food group gradually increased, and the weight of the starvation group gradually decreased (Figures 7B and 7C). Microbial contamination was not observed in the intestines of *G. mellonella* at 15 days after antibiotic treatment (Figure 7D).

On the other hand, in the case of nutrition-rich food treatment on the 15th day, the weight of the antibiotic treatment group (mean, 33.2 mg) was decreased compared to the control treatment group (mean, 41.5 mg). Therefore, although the intestinal microbiota has the potential to play a role in the digestion of nutrition-rich foods, which are complex nutrients, the role of the intestinal microbiota in the decomposition of PE is not as important as that of beeswax degradation.

To investigate the formation of intermediates of PE metabolism, including hydrocarbons and fatty acids, long-chain fatty acids from the midgut and frass of *G. mellonella* larvae were profiled by GC-MS. PE was used as a control (Figure 7D).

Long-chain hydrocarbons such as heptadecane, octadecane, eicosane, docosane, and tetracosane were found in PE (Figure 7D). In PE fed with intestinal microbiota, hexadecanoic acid and 9-octadecanoic acid were generated as long-chain fatty acids (Figure 7D). The peak of long-chain hydrocarbons was decreased in frass. In addition, long-chain fatty acid was not detected in the intestines (Figure 7D). The content of these two fatty acids was not significantly affected in the intestinal-microbiota-deficient intestine. However, in frass, a difference in the peak between the metabolites was found in the control group. This indicates that PE is metabolized by partial interaction with intestinal microorganisms (Figure 7D). At 15 days after antibiotic treatment, intestinal microbiota was no longer detected by culture-dependent methods (Figure 7E).

DISCUSSION

This is a study of long-chain fatty acid decomposition via beeswax metabolism using genetic and biochemical approaches in the insect. In the feeding experiments using beeswax and PE, larvae weights were maintained regardless of presence or absence of the intestinal microbiota in comparison with starvation. On the other hand, the weights of the insects fed nutrition-rich food were decreased when the intestinal microbiota was absent. These results suggest that the microbiota does not play a role in the metabolism of long-chain hydrocarbon wax but does play a role in the nutrition-rich diets of the waxworms from a local source. Furthermore, the presence of octadecanoic acid, *cis*-vaccenic acid, and palmitic acid in beeswax-fed *G. mellonella* lacking intestinal microbiota suggested the possible biodegradation of long-chain fatty acids from beeswax by the host. These results led us to establish a high-quality reference genome of intestinal-microbiota-free *G. mellonella* for genetic analysis of the evolution of wax degradation. Whole-genome data revealed a significant expansion of hydrolase activity in *G. mellonella* that could assist the digestion of long-chain hydrocarbon wax in honeycomb. In addition, gene families related to lipid metabolites and transport systems are enriched in *G. mellonella* compared with other Lepidoptera species (Table S5). Expansion of these gene families is consistent with the evolution of wax digestion and absorption of the resulting short-chain fatty acid degradation products.

This study investigated the potential degradability of PE by assessing the genome of *G. mellonella* and the mechanism of long-chain hydrocarbon wax degradation at the genetic level. When the intestinal microbiota was removed by antibiotic treatment and beeswax alone was supplied as the sole nutrient source, *G. mellonella* survived for 15 days and underwent a normal life cycle. Thus, *G. mellonella* larvae appeared to degrade long-chain hydrocarbon wax without assistance from the intestinal microbiota. Additionally, the same long-chain fatty acids and associated metabolites were detected in the presence and absence of the intestinal microbiota, further suggesting that

(D) Insect groups with (treated with PBS) and without (treated with antibiotics) intestinal microbiota displayed intestinal component profiles identical to those of nutrition-rich food (NR) and low-density polyethylene (LDPE) diets. Peak identities are as follows: 1, hexadecane; 2, octadecane; 3, eicosane; 4, docosane; 5, tetracosane; 6, hexadecanoic acid, methyl ester; and 7, 9-octadecenoic acid, methyl ester.
(E) Bacterial contamination in antibiotic-treated intestine was investigated by the culture method. For the culture method, after 15 days of antibiotic treatment, intestines were removed and diluted in TSA media. Differences in frass type between nutrition-rich- and polyethylene-fed *G. mellonella* larvae are shown.

the intestinal microbiota does not produce long-chain fatty acids or long-chain ethanol by decomposing long-chain hydrocarbon wax. Beeswax contains 14% long-chain hydrocarbons, which are also a major component of PE (Benson et al., 1975; Downs et al., 2002; Gary et al., 1980; Tulloch, 1980), the most common plastic that consists largely of high-molecular-weight hydrocarbons. Therefore, an understanding of the hydrolytic metabolism mechanism in beeswax could assist the development of a metabolism strategy for PE. Recently, Brandon et al. (2018) investigated the biodegradation of PE by yellow mealworms. Yang and co-workers found that mealworms performed PS degradation dependence on gut microbiota (Yang et al., 2015a, 2015b, 2018a, 2018b). Most studies focused on the isolation of intestinal microbiota. However, this method has failed to provide significant insight into the role of host and intestinal microbiota metabolic processes. Therefore, we searched for solid evidence of wax degradation by hosts and intestinal microbiota using *G. mellonella*, which feeds on PE-like long-chain hydrocarbon beeswax. *T. molitor* larvae (mealworms) which grow on wheat bran, grain, and various vegetables, likely have different enzymatic system and gut microbiota from those of *G. mellonella*. Therefore, both may behave differently for biodegradation of plastics such as PE and PS.

Expansion of esterase and lipase genes in *G. mellonella* implies the possible conversion of long-chain fatty acid forms of $C_{15}H_{31}COONa$ via breakage of ester bonds in beeswax (Benson et al., 1975; Downs et al., 2002). To decompose long-chain hydrocarbons and use them as an energy source, hydroxyl groups are introduced via monooxygenase reactions catalyzed by CYP enzymes (Ortiz de Montellano, 2010). In the *G. mellonella* genome, the CYP9 gene family is expanded (Table S10). Expansion of the CYP gene family can promote the formation of alcohols by introducing hydroxyl groups into hydrocarbons (Ortiz de Montellano, 2010). Alcohols resulting from monooxygenase-catalyzed hydrolysis by CYPs are subjected to alcohol oxidation and beta oxidation that generate butanoyl-CoA and propanoyl-CoA byproducts, which are subsequently converted to acetyl-CoA by butanoate and propanoate metabolism prior to use as an energy source (Figure 5B; Gatter et al., 2014). In addition, expansion of fatty acid metabolism, fatty acid biosynthesis, and fatty acid degradation pathways indicates metabolism of wax into $C_{15}H_{31}COONa$ short-chain fatty acids as an energy source (Houten and Wanders, 2010). Contraction of genes related to sodium:potassium-exchanging ATPase activity, potassium transport ATPase activity, and potassium ions in *G. mellonella* regulates acidosis *in vivo* (Aronson and Giebisch, 2011).

KEGG pathway analysis of the transcriptome data revealed that hydrocarbon metabolism and carbon metabolism were activated in beeswax-fed *G. mellonella* fat body tissue. In addition, fatty acid degradation and fatty acid metabolism were more active in beeswax-fed *G. mellonella* fat bodies than in those of larvae fed a nutrition-rich diet without beeswax (Table S8). This indicates that many gene families are activated for long-chain fatty acid metabolism and accumulation through wax degradation in *G. mellonella*. This genetic approach demonstrates that triacontanyl palmitate is formed from beeswax by esterases and lipases, and energy is derived from short-chain fatty acids following degradation of ester bonds and carbon-carbon single bonds.

Interestingly, the long-chain fatty acid content was similar in the larval gut with and without intestinal microbiota (Figure 2), suggesting that the intestinal microbiota does not play a primary role in the degradation of wax into long-chain fatty acids. However, the observed enrichment of metabolic processes and synthesis of secondary metabolites in intestinal microbiota grown in the presence of beeswax suggests that the intestinal microbiota may participate in the degradation process after long-chain fatty acid production. Therefore, our results indicate that long-chain hydrocarbon wax is first depolymerized or hydrolyzed into long-chain fatty acids by the host and that the intestinal microbiota are secondary wax degraders. The expression of short-chain fatty acids metabolism genes derived from beeswax in the intestinal microbiota may suggest a nutritional competitive relationship with hosts as well as secondary wax degraders.

Other functions of intestinal microbiota may be related to immune functions and/or other ecological roles of *G. mellonella* (Buffie and Pamer, 2013; Ceja-Navarro et al., 2015; Shao et al., 2017). However, little is known about the mechanisms through which the intestinal microbiota in gastrointestinal tracts affects the insect hosts. Currently, we evaluated the microbial role on innate immunity.

In this study, we deduced a high-quality greater wax moth genome using PacBio long-read sequencing data. The great wax moth is a notorious insect pest that damages beehive farms worldwide, contributing to honeybee colony collapse disorder (Burges and Bailey, 1968; Oldroyd, 2007), but the ability of this insect to digest beeswax and PE is very interesting. We discovered that *G. mellonella* produces long-chain fatty acids from long-chain hydrocarbon wax without microbial assistance. Although the intestinal microbiota does not play a major role in long-chain hydrocarbon wax and PE degradation, we cannot rule out the significance of the intestinal microbiota in host physiology and immunity. We hypothesize that the great wax moth uses a complete set of enzymes to degrade both natural and nutrition-rich lipids. Exploration of wax metabolism in *G. mellonella* at the genetic and enzymatic levels, and integration of the findings, may assist the development of efficient biological degradation processes for currently nondegradable PE pollutants.

STAR★METHODS

Detailed methods are provided in the online version of this paper and include the following:

- KEY RESOURCES TABLE
- CONTACT FOR REAGENT AND RESOURCE SHARING
- EXPERIMENTAL MODEL AND SUBJECT DETAILS
  - Insect rearing and sampling
- METHOD DETAILS
  - Antibiotic treatment
  - Measuring larval weight following feeding on beeswax, PE or an artificial diet
  - Honey and wax diets
  - GC-MS quantification of fatty acids

SUPPLEMENTAL INFORMATION

Supplemental Information can be found with this article online at https://doi.org/10.1016/j.celrep.2019.02.018.

ACKNOWLEDGMENTS

This research was supported by grants from the Woo Jang-Choon Project (PJ01093904) of the Rural Development Administration, the Korea Research Institute of Bioscience and Biotechnology (KRIBB) Initiative Program of South Korea. This work was also supported by the 2015 Research Fund (1.150014.01) of the Ulsan National Institute of Science & Technology (UNIST) and the Software Convergence Technology Development Program through the Ministry of Science, ICT and Future Planning (S0503-17-1007). We thank Hae Ran Lee and Myoung joo Riu at the Infectious Disease Research Center, KRIBB, for experimental assistance.

AUTHOR CONTRIBUTIONS

C.-M.R. designed the study. H.G.K., H.H.K., and J.-h.C. performed all experiments, with help from S.H.L., who helped with *in vitro* experiments, *in vivo* treatments, and gut tissue collection. C.-M.R. and J.B. contributed to scientific discussion and guided the direction of the project. C.-M.R., H.G.K., and H.H.K. wrote the manuscript. Bioinformatics data processing and analyses were carried out by J.J., H.H.K., H.-M.K., S.J., S.G.P., H.G.K., H.H.K., J.C., and J.B.

DECLARATION OF INTERESTS

H.H.K. and J.J. are employees and J.B. is on the scientific advisory board of Clinomics. The remaining authors declare no competing interests.

Received: September 16, 2018
Revised: December 24, 2018
Accepted: February 6, 2019
Published: February 26, 2019

REFERENCES

Albertsson, A.C., and Karlsson, S. (1988). The three stages in degradation of polymers–polyethylene as a model substance. J. Appl. Polym. Sci. *35*, 1289–1302.

Albertsson, A.C., Andersson, S.O., and Karlsson, S. (1987). The mechanism of biodegradation of polyethylene. Polym. Degrad. Stabil. *18*, 73–87.

Albertsson, A.C., Erlandsson, B., Hakkarainen, M., and Karlsson, S. (1998). Molecular weight changes and polymeric matrix changes correlated with the formation of degradation products in biodegraded polyethylene. J. Environ. Polym. Degrad. *6*, 187–195.

Ammala, A., Bateman, S., Dean, K., Petinakis, E., Sangwan, P., Wong, S., Yuan, Q., Yu, L., Patrick, C., and Leong, K.H. (2011). An overview of degradable and biodegradable polyolefins. Prog. Polym. Sci. *36*, 1015–1049.

Aronson, P.S., and Giebisch, G. (2011). Effects of pH on potassium: new explanations for old observations. J. Am. Soc. Nephrol. *22*, 1981–1989.

Artham, T., Sudhakar, M., Venkatesan, R., Madhavan Nair, C., Murty, K.V.G.K., and Doble, M. (2009). Biofouling and stability of synthetic polymers in sea water. Int. Biodeterior. Biodegradation *63*, 884–890.

Attwood, T.K., and Beck, M.E. (1994). PRINTS—a protein motif fingerprint database. Protein Eng. *7*, 841–848.

Bairoch, A., and Apweiler, R. (2000). The SWISS-PROT protein sequence database and its supplement TrEMBL in 2000. Nucleic Acids Res. *28*, 45–48.

Benson, G. (1999). Tandem repeats finder: a program to analyze DNA sequences. Nucleic Acids Res. *27*, 573–580.

Benson, A.A., Patton, J.S., and Field, C.E. (1975). Wax digestion in a Crown-of-Thorns starfish. Comp. Biochem. Physiol. B *52*, 339–340.

Besemer, J., and Borodovsky, M. (2005). GeneMark: web software for gene finding in prokaryotes, eukaryotes and viruses. Nucleic Acids Res. *33*, W451–W454.

Brandon, A.M., Gao, S.-H., Tian, R., Ning, D., Yang, S.-S., Zhou, J., Wu, W.-M., and Criddle, C.S. (2018). Biodegradation of polyethylene and plastic mixtures in mealworms (larvae of *Tenebrio molitor*) and effects on the gut microbiome. Environ. Sci. Technol. *52*, 6526–6533.

Bru, C., Courcelle, E., Carrère, S., Beausse, Y., Dalmar, S., and Kahn, D. (2005). The ProDom database of protein domain families: more emphasis on 3D. Nucleic Acids Res. *33*, D212–D215.

Buffie, C.G., and Pamer, E.G. (2013). Microbiota-mediated colonization resistance against intestinal pathogens. Nat. Rev. Immunol. *13*, 790–801.

Burges, H.D., and Bailey, L. (1968). Control of the greater and lesser wax moths (*Galleria mellonella* and *Achroia grisella*) with *Bacillus thuringiensis*. J. Invertebr. Pathol. *11*, 184–195.

Camacho, C., Coulouris, G., Avagyan, V., Ma, N., Papadopoulos, J., Bealer, K., and Madden, T.L. (2009). BLAST+: architecture and applications. BMC Bioinformatics *10*, 421.

Cantarel, B.L., Korf, I., Robb, S.M., Parra, G., Ross, E., Moore, B., Holt, C., Sánchez Alvarado, A., and Yandell, M. (2008). MAKER: an easy-to-use annotation pipeline designed for emerging model organism genomes. Genome Res. *18*, 188–196.

Capella-Gutiérrez, S., Silla-Martínez, J.M., and Gabaldón, T. (2009). trimAl: a tool for automated alignment trimming in large-scale phylogenetic analyses. Bioinformatics *25*, 1972–1973.

Ceja-Navarro, J.A., Vega, F.E., Karaoz, U., Hao, Z., Jenkins, S., Lim, H.C., Kosina, P., Infante, F., Northen, T.R., and Brodie, E.L. (2015). Gut microbiota mediate caffeine detoxification in the primary insect pest of coffee. Nat. Commun. *6*, 7618.

Chevallier, A., and Garel, J.P. (1982). Differential synthesis rates of tRNA species in the silk gland of Bombyx mori are required to promote tRNA adaptation to silk messages. Eur. J. Biochem. *124*, 477–482.

Chin, C.S., Alexander, D.H., Marks, P., Klammer, A.A., Drake, J., Heiner, C., Clum, A., Copeland, A., Huddleston, J., Eichler, E.E., et al. (2013). Nonhybrid, finished microbial genome assemblies from long-read SMRT sequencing data. Nat. Methods *10*, 563–569.

Downs, C.T., van Dyk, R.J., and Iji, P. (2002). Wax digestion by the lesser honeyguide Indicator minor. Comp. Biochem. Physiol. A Mol. Integr. Physiol. *133*, 125–134.

Edgar, R.C. (2004). MUSCLE: multiple sequence alignment with high accuracy and high throughput. Nucleic Acids Res. *32*, 1792–1797.

El Aidy, S., Derrien, M., Merrifield, C.A., Levenez, F., Doré, J., Boekschoten, M.V., Dekker, J., Holmes, E., Zoetendal, E.G., van Baarlen, P., et al. (2013). Gut bacteria-host metabolic interplay during conventionalisation of the mouse germfree colon. ISME J. *7*, 743–755.

Ferdinandusse, S., Denis, S., Hogenhout, E.M., Koster, J., van Roermund, C.W., IJlst, L., Moser, A.B., Wanders, R.J., and Waterham, H.R. (2007). Clinical, biochemical, and mutational spectrum of peroxisomal acyl-coenzyme A oxidase deficiency. Hum. Mutat. *28*, 904–912.

Freed, D.N., Aldana, R., Weber, J.A., and Edwards, J.S. (2017). The Sentieon Genomics Tools: a fast and accurate solution to variant calling from next-generation sequence data. bioRxiv. https://doi.org/10.1101/115717.

Gary, J.B., Arthur, J.C., and Stephen, R. (1980). Biosynthesis of wax in the honeybee, *Apis mellifera* L. Insect Biochem. *10*, 313–321.

Gatter, M., Förster, A., Bär, K., Winter, M., Otto, C., Petzsch, P., Ježková, M., Bahr, K., Pfeiffer, M., Matthäus, F., and Barth, G. (2014). A newly identified fatty alcohol oxidase gene is mainly responsible for the oxidation of long-chain ω-hydroxy fatty acids in Yarrowia lipolytica. FEMS Yeast Res. *14*, 858–872.

Grabherr, M.G., Haas, B.J., Yassour, M., Levin, J.Z., Thompson, D.A., Amit, I., Adiconis, X., Fan, L., Raychowdhury, R., Zeng, Q., et al. (2011). Full-length transcriptome assembly from RNA-seq data without a reference genome. Nat. Biotechnol. *29*, 644–652.

Han, M.V., Thomas, G.W., Lugo-Martinez, J., and Hahn, M.W. (2013). Estimating gene gain and loss rates in the presence of error in genome assembly and annotation using CAFE 3. Mol. Biol. Evol. *30*, 1987–1997.

Hillman, E.T., Lu, H., Yao, T., and Nakatsu, C.H. (2017). Microbial ecology along the gastrointestinal tract. Microbes Environ. *32*, 300–313.

Houten, S.M., and Wanders, R.J.A. (2010). A general introduction to the biochemistry of mitochondrial fatty acid β-oxidation. J. Inherit. Metab. Dis. *33*, 469–477.

Hsiao, W.W.L., Metz, C., Singh, D.P., Roth, J., and Jesse Roth, M.D. (2008). The microbes of the intestine: an introduction to their metabolic and signaling capabilities. Endocrinol. Metab. Clin. North Am. *37*, 857–871.

Huang, A.H., Moreau, R.A., and Liu, K.D. (1978). Development and properties of a wax ester hydrolase in the cotyledons of jojoba seedlings. Plant Physiol. *61*, 339–341.

Hulo, N., Bairoch, A., Bulliard, V., Cerutti, L., De Castro, E., Langendijk-Genevaux, P.S., Pagni, M., and Sigrist, C.J. (2006). The PROSITE database. Nucleic Acids Res. *34*, D227–D230.

Huson, D.H., Beier, S., Flade, I., Górska, A., El-Hadidi, M., Mitra, S., Ruscheweyh, H.J., and Tappu, R. (2016). MEGAN Community Edition: interactive exploration and analysis of large-scale microbiome sequencing data. PLoS Comput. Biol. *12*, e1004957.

Jones, P.H., Prasad, D., Heskins, M., Morgan, M.H., and Guillet, J.E. (1974). Biodegradability of photodegraded polymers. I. Development of experimental procedures. Environ. Sci. Technol. *8*, 919–923.

Jurka, J., Kapitonov, V.V., Pavlicek, A., Klonowski, P., Kohany, O., and Walichiewicz, J. (2005). Repbase Update, a database of eukaryotic repetitive elements. Cytogenet. Genome Res. *110*, 462–467.

Kambhampati, S., and Rai, K.S. (1991). Patterns of morphometric and allozyme variation in *Aedes albopictus*. Entomol. Exp. Appl. *60*, 193–201.

Kent, W.J. (2002). BLAT–the BLAST-like alignment tool. Genome Res. *12*, 656–664.

Kim, D., and Salzberg, S.L. (2011). TopHat-Fusion: an algorithm for discovery of novel fusion transcripts. Genome Biol. *12*, R72.

Kim, D., Pertea, G., Trapnell, C., Pimentel, H., Kelley, R., and Salzberg, S.L. (2013). TopHat2: accurate alignment of transcriptomes in the presence of insertions, deletions and gene fusions. Genome Biol. *14*, R36.

Klein, A.M., Vaissière, B.E., Cane, J.H., Steffan-Dewenter, I., Cunningham, S.A., Kremen, C., and Tscharntke, T. (2007). Importance of pollinators in changing landscapes for world crops. Proc. Biol. Sci. *274*, 303–313.

Korf, I. (2004). Gene finding in novel genomes. BMC Bioinformatics *5*, 59.

Kumar, S., Stecher, G., and Tamura, K. (2016). MEGA7: Molecular Evolutionary Genetics Analysis version 7.0 for bigger datasets. Mol. Biol. Evol. *33*, 1870–1874.

Kwadha, C.A., Ong'amo, G.O., Ndegwa, P.N., Raina, S.K., and Fombong, A.T. (2017). The Biology and control of the greater wax moth, *Galleria mellonella*. Insects *8*, 16.

Labandeira, C.C. (1997). Insect mouthparts: ascertaining the paleobiology of insect feeding strategies. Annu. Rev. Ecol. Syst. *28*, 153–193.

Larkin, M.A., Blackshields, G., Brown, N.P., Chenna, R., McGettigan, P.A., McWilliam, H., Valentin, F., Wallace, I.M., Wilm, A., Lopez, R., et al. (2007). Clustal W and Clustal X version 2.0. Bioinformatics *23*, 2947–2948.

Li, H., and Durbin, R. (2009). Fast and accurate short read alignment with Burrows-Wheeler transform. Bioinformatics *25*, 1754–1760.

Li, L., Stoeckert, C.J., Jr., and Roos, D.S. (2003). OrthoMCL: identification of ortholog groups for eukaryotic genomes. Genome Res. *13*, 2178–2189.

Li, R., Fan, W., Tian, G., Zhu, H., He, L., Cai, J., Huang, Q., Cai, Q., Li, B., Bai, Y., et al. (2010). The sequence and de novo assembly of the giant panda genome. Nature *463*, 311–317.

Mahdiyah, D., and Mukti, B.H. (2013). Isolation of polyethylene plastic degrading-bacteria. Biosci. Int. *2*, 29–32.

Majoros, W.H., Pertea, M., and Salzberg, S.L. (2004). TigrScan and GlimmerHMM: two open source ab initio eukaryotic gene-finders. Bioinformatics *20*, 2878–2879.

Martel, A.C., Zeggane, S., Drajnudel, P., Faucon, J.P., and Aubert, M. (2006). Tetracycline residues in honey after hive treatment. Food Addit. Contam. *23*, 265–273.

McFall-Ngai, M., Hadfield, M.G., Bosch, T.C., Carey, H.V., Domazet-Lošo, T., Douglas, A.E., Dubilier, N., Eberl, G., Fukami, T., Gilbert, S.F., et al. (2013). Animals in a bacterial world, a new imperative for the life sciences. Proc. Natl. Acad. Sci. USA *110*, 3229–3236.

Mi, H., Lazareva-Ulitsky, B., Loo, R., Kejariwal, A., Vandergriff, J., Rabkin, S., Guo, N., Muruganujan, A., Doremieux, O., Campbell, M.J., et al. (2005). The PANTHER database of protein families, subfamilies, functions and pathways. Nucleic Acids Res. *33*, D284–D288.

Moriya, Y., Itoh, M., Okuda, S., Yoshizawa, A.C., and Kanehisa, M. (2007). KAAS: an automatic genome annotation and pathway reconstruction server. Nucleic Acids Res. *35*, W182–W185.

Nkwachukwu, O.I., Chima, C.H., Ikenna, A.O., and Albert, L. (2013). Focus on potential environmental issues on plastic world towards a sustainable plastic recycling in developing countries. J. Industrial Chem. *4*, 34.

Nowack, B., and Bucheli, T.D. (2007). Occurrence, behavior and effects of nanoparticles in the environment. Environ. Pollut. *150*, 5–22.

Oaxaca-Castillo, D., Andreoletti, P., Vluggens, A., Yu, S., van Veldhoven, P.P., Reddy, J.K., and Cherkaoui-Malki, M. (2007). Biochemical characterization of two functional human liver acyl-CoA oxidase isoforms 1a and 1b encoded by a single gene. Biochem. Biophys. Res. Commun. *360*, 314–319.

Ohtake, Y., Kobayashi, T., Asabe, H., Murakami, N., and Ono, K. (1998). Oxidative degradation and molecular weight change of LDPE buried under bioactive soil for 32–37 years. J. Appl. Polym. Sci. *70*, 1643–1648.

Oldroyd, B.P. (1999). Coevolution while you wait: *Varroa jacobsoni*, a new parasite of western honeybees. Trends Ecol. Evol. *14*, 312–315.

Oldroyd, B.P. (2007). What's killing American honey bees? PLoS Biol. *5*, e168.

Ortiz de Montellano, P.R. (2010). Hydrocarbon hydroxylation by cytochrome P450 enzymes. Chem. Rev. *110*, 932–948.

Parra, G., Blanco, E., and Guigó, R. (2000). GeneID in Drosophila. Genome Res. *10*, 511–515.

Pathak, V.M. (2017). Review on the current status of polymer degradation: a microbial approach. Bioresour. Bioprocess. *4*, 15.

Pegram, J.E., and Andrady, A.L. (1989). Outdoor weathering of selected polymeric materials under marine exposure conditions. Polym. Degrad. Stabil. *26*, 333–345.

Ponting, C.P., Schultz, J., Milpetz, F., and Bork, P. (1999). SMART: identification and annotation of domains from signalling and extracellular protein sequences. Nucleic Acids Res. *27*, 229–232.

Price, A.L., Jones, N.C., and Pevzner, P.A. (2005). De novo identification of repeat families in large genomes. Bioinformatics *21* (*Suppl 1*), i351–i358.

Punta, M., Coggill, P.C., Eberhardt, R.Y., Mistry, J., Tate, J., Boursnell, C., Pang, N., Forslund, K., Ceric, G., Clements, J., et al. (2012). The Pfam protein families database. Nucleic Acids Res. *40*, D290–D301.

Qu, Q., Zeng, F., Liu, X., Wang, Q.J., and Deng, F. (2016). Fatty acid oxidation and carnitine palmitoyltransferase I: emerging therapeutic targets in cancer. Cell Death Dis. *7*, e2226.

Ramarao, N., Nielsen-Leroux, C., and Lereclus, D. (2012). The insect *Galleria mellonella* as a powerful infection model to investigate bacterial pathogenesis. J. Vis. Exp. *70*, 4392.

Regert, M., Colinart, S., Degrand, L., and Decavallas, O. (2001). Chemical alteration and use of beeswax through time: accelerated ageing tests and analysis of archaeological samples from various environmental contexts. Archaeometry *43*, 549–569.

Roberts, A., Pimentel, H., Trapnell, C., and Pachter, L. (2011). Identification of novel transcripts in annotated genomes using RNA-Seq. Bioinformatics *27*, 2325–2329.

Rowland, I., Gibson, G., Heinken, A., Scott, K., Swann, J., Thiele, I., and Tuohy, K. (2018). Gut microbiota functions: metabolism of nutrients and other food components. Eur. J. Nutr. *57*, 1–24.

Roy, P.K., Hakkarainen, M., Varma, I.K., and Albertsson, A.C. (2011). Degradable polyethylene: fantasy or reality. Environ. Sci. Technol. *45*, 4217–4227.

Shah, A.A., Hasan, F., Hameed, A., and Ahmed, S. (2008). Biological degradation of plastics: a comprehensive review. Biotechnol. Adv. *26*, 246–265.

Shao, Y., Chen, B., Sun, C., Ishida, K., Hertweck, C., and Boland, W. (2017). Symbiont-derived antimicrobials contribute to the control of the Lepidopteran gut microbiota. Cell Chem. Biol. *24*, 66–75.

Simão, F.A., Waterhouse, R.M., Ioannidis, P., Kriventseva, E.V., and Zdobnov, E.M. (2015). BUSCO: assessing genome assembly and annotation completeness with single-copy orthologs. Bioinformatics *31*, 3210–3212.

Singh, J., and Gupta, K. (2014). Screening and identification of low density polyethylene (LDPE) degrading soil fungi isolated from polythene polluted sites around Gwalior city (MP). Int. Curr. Microbiol. Appl. Sci. *3*, 443–448.

Slater, G.S., and Birney, E. (2005). Automated generation of heuristics for biological sequence comparison. BMC Bioinformatics *6*, 31.

St Pierre, S.E., Ponting, L., Stefancsik, R., and McQuilton, P.; FlyBase Consortium (2014). FlyBase 102–advanced approaches to interrogating FlyBase. Nucleic Acids Res. *42*, D780–D788.

Stamatakis, A. (2014). RAxML version 8: a tool for phylogenetic analysis and post-analysis of large phylogenies. Bioinformatics *30*, 1312–1313.

Stanke, M., Keller, O., Gunduz, I., Hayes, A., Waack, S., and Morgenstern, B. (2006). AUGUSTUS: ab initio prediction of alternative transcripts. Nucleic Acids Res. *34*, W435–W439.

Tokiwa, Y., Calabia, B.P., Ugwu, C.U., and Aiba, S. (2009). Biodegradability of plastics. Int. J. Mol. Sci. *10*, 3722–3742.

Trapnell, C., Hendrickson, D.G., Sauvageau, M., Goff, L., Rinn, J.L., and Pachter, L. (2013). Differential analysis of gene regulation at transcript resolution with RNA-seq. Nat. Biotechnol. *31*, 46–53.

Tulloch, A.P. (1980). Beeswax-composition and analysis. Bee World *61*, 47–62.

UniProt Consortium (2012). Reorganizing the protein space at the Universal Protein Resource (UniProt). Nucleic Acids Res. *40*, D71–D75.

Wilkes, R.A., and Aristilde, L. (2017). Degradation and metabolism of synthetic plastics and associated products by Pseudomonas sp.: capabilities and challenges. J. Appl. Microbiol. *123*, 582–593.

Wu, W.-M., Yang, J., and Criddle, C.S. (2017). Microplastics pollution and reduction strategies. Front. Environ. Sci. Eng. *11*, 6.

Xia, Q., Zhou, Z., Lu, C., Cheng, D., Dai, F., Li, B., Zhao, P., Zha, X., Cheng, T., Chai, C., et al.; Biology Analysis Group (2004). A draft sequence for the genome of the domesticated silkworm (Bombyx mori). Science *306*, 1937–1940.

Yang, Z. (2007). PAML 4: phylogenetic analysis by maximum likelihood. Mol. Biol. Evol. *24*, 1586–1591.

Yang, J., Yang, Y., Wu, W.M., Zhao, J., and Jiang, L. (2014). Evidence of polyethylene biodegradation by bacterial strains from the guts of plastic-eating waxworms. Environ. Sci. Technol. *48*, 13776–13784.

Yang, Y., Yang, J., Wu, W.-M., Zhao, J., Song, Y., Gao, L., Yang, R., and Jiang, L. (2015a). Biodegradation and mineralization of polystyrene by plastic-eating mealworms: part 1. Chemical and physical characterization and isotopic tests. Environ. Sci. Technol. *49*, 12080–12086.

Yang, Y., Yang, J., Wu, W.-M., Zhao, J., Song, Y., Gao, L., Yang, R., and Jiang, L. (2015b). Biodegradation and mineralization of polystyrene by plastic-eating mealworms: part 2. Role of gut microorganisms. Environ. Sci. Technol. *49*, 12087–12093.

Yang, S.-S., Brandon, A.M., Andrew Flanagan, J.C., Yang, J., Ning, D., Cai, S.Y., Fan, H.Q., Wang, Z.Y., Ren, J., Benbow, E., et al. (2018a). Biodegradation of polystyrene wastes in yellow mealworms (larvae of *Tenebrio molitor* Linnaeus): Factors affecting biodegradation rates and the ability of polystyrene-fed larvae to complete their life cycle. Chemosphere *191*, 979–989.

Yang, S.-S., Wu, W.M., Brandon, A.M., Fan, H.Q., Receveur, J.P., Li, Y., Wang, Z.Y., Fan, R., McClellan, R.L., Gao, S.H., et al. (2018b). Ubiquity of polystyrene digestion and biodegradation within yellow mealworms, larvae of *Tenebrio molitor* Linnaeus (Coleoptera: Tenebrionidae). Chemosphere *212*, 262–271.

Zdobnov, E.M., and Apweiler, R. (2001). InterProScan—an integration platform for the signature-recognition methods in InterPro. Bioinformatics *17*, 847–848.

Zettler, E.R., Mincer, T.J., and Amaral-Zettler, L.A. (2013). Life in the "plastisphere": microbial communities on plastic marine debris. Environ. Sci. Technol. *47*, 7137–7146.

Zhang, J., Nielsen, R., and Yang, Z. (2005). Evaluation of an improved branch-site likelihood method for detecting positive selection at the molecular level. Mol. Biol. Evol. *22*, 2472–2479.

STAR★METHODS

KEY RESOURCES TABLE

REAGENT or RESOURCE	SOURCE	IDENTIFIER
Chemicals, Peptides, and Recombinant Proteins		
Beeswax	Samchun pure chemical	Cat# B1180
Low density PE	ThermoFisher Scientific	Cat# A10239
Critical Commercial Assays		
TRIzol reagent	Invitrogen	Cat# 15596026
Software and Algorithms		
TopHat (v2.0.11)	Kim and Salzberg, 2011	https://ccb.jhu.edu/software/tophat/index.shtml
Cufflinks (v2.12.0)	Trapnell et al., 2013	https://github.com/cole-trapnell-lab/cufflinks/
Falcon Assembler (v0.3.0)	Chin et al., 2013	https://pb-falcon.readthedocs.io/en/latest/
BWA-MEN	Li and Durbin, 2009	http://bio-bwa.sourceforge.net/index.shtml
Sentieon	Freed et al., 2017	https://www.sentieon.com/products/
Exonerate software (v2.2.0)	Slater and Birney, 2005	https://www.ebi.ac.uk/about/vertebrate-genomics/software/exonerate
Program to Assemble Spliced Alignment	Li et al., 2010	https://github.com/PASApipeline/PASApipeline/wiki
Trinity (v2.3.0)	Grabherr et al., 2011	https://github.com/trinityrnaseq/trinityrnaseq/releases
AUGUSTUS (v3.0.3)	Stanke et al., 2006	http://bioinf.uni-greifswald.de/augustus/
Maker (v2.31.9)	Cantarel et al., 2008	https://wiki.cyverse.org/wiki/display/TUT/MAKER-P_2.31.9+Atmosphere+Tutorial
SNAP (v2013-11-29)	Korf, 2004	http://snap.cs.berkeley.edu/
GlimmerHMM (v3.0.4)	Majoros et al., 2004	https://ccb.jhu.edu/software/glimmerhmm/
Genemark (v4.32)	Besemer and Borodovsky, 2005	http://exon.gatech.edu/GeneMark/
GeneID (v1.4)	Parra et al., 2000	http://genome.crg.es/software/geneid/
Tandem Repeats Finder (v4.07b)	Benson, 1999	https://tandem.bu.edu/trf/trf.html
Repbase (v19.03)	Jurka et al., 2005	https://www.girinst.org/repbase/
RepeatModeler (v1.0.7)	Price et al., 2005	http://www.repeatmasker.org/RepeatModeler/
Blat	Kent, 2002	https://genome.ucsc.edu/FAQ/FAQblat.html
BUSCO software	Simão et al., 2015	https://busco.ezlab.org/
SwissProt	UniProt Consortium, 2012	https://www.uniprot.org/
TrEMBL	Bairoch and Apweiler, 2000	http://www.bioinfo.pte.hu/more/TrEMBL.htm
FlyBase	St Pierre et al., 2014	https://flybase.org/
InterProScan (v5.13)	Zdobnov and Apweiler, 2001	https://www.ebi.ac.uk/interpro/search/sequence-search
Pfam	Punta et al., 2012	https://pfam.xfam.org/
PATHER	Mi et al., 2005	http://www.pantherdb.org/
ProDom	Bru et al., 2005	http://prodom.prabi.fr/prodom/current/html/home.php
PROSITE	Hulo et al., 2006	https://prosite.expasy.org/
OrthoMCL (v2.0.9)	Li et al., 2003	http://orthomcl.org/orthomcl/
MUSCLE	Edgar, 2004	https://www.ebi.ac.uk/Tools/msa/muscle/
TrimAl	Capella-Gutiérrez et al., 2009	http://trimal.cgenomics.org/
MEGA7	Kumar et al., 2016	https://www.megasoftware.net/
PAML 4.5 package	Yang, 2007	http://abacus.gene.ucl.ac.uk/software/paml.html
BLASTx (v2.2.28+)	Camacho et al., 2009	https://blast.ncbi.nlm.nih.gov/Blast.cgi
Megan6	Huson et al., 2016	https://ab.inf.uni-tuebingen.de/software/megan6
Deposited Data		
Genome sequencing Raw and analyzed data	This paper	SUB2718188
RNA sequencing Raw and analyzed data	This paper	PRJNA386430

CONTACT FOR REAGENT AND RESOURCE SHARING

Further information and requests for resources and reagents should be directed to and will be fulfilled by the Lead Contact, Choongmin Ryu (cmryu@kribb.re.kr).

EXPERIMENTAL MODEL AND SUBJECT DETAILS

Insect rearing and sampling

Galleria mellonella larvae were obtained from ECOWIN Co. (Andong, S. Korea). The each 200 larvae were kept in the dark in 6.5-l plastic cage (31.5 X 23 X 11.5 cm, Lock&Lock Co.Ltd., S. Korea) filled with nutrition-rich food at 30°C. The nutrition-rich food was composed of 300 g of wheat bran, 300 g of rice bran, 2.25 g of yeast extract, 1 g of $CaCO_3$, 125 mL of glycerol, 87.5 mL of honey, and 300 mg of vitamin B complex per 1 L of medium. The ingredients were mixed and unused food was stored at 4°C. The nutrition-rich food has been replaced at least once a week, except when more is added to the container. About 2-3 months later, the larvae were converted into pupae, and about 100 pupae were moved to a new 6.5-l plastic cage without food. The eggs of the next generation were obtained from the adults in the transferred 6.5-l plastic cage. Eggs hatched within 3 days, and small larvae began to develop upon feeding with a nutrition-rich diet.

4^{th} instar *G. mellonella* individuals were collected and rinsed with 100% ethanol and sterile water. Larvae were removed and rinsed three times in 100% ethanol, then stored in 100% ethanol until further processing. All larval gut samples were taken in triplicate.

METHOD DETAILS

Antibiotic treatment

For antibiotic treatments, *G. mellonella* larvae were starved for 4 h then subjected to force-feeding twice for 12 h with 10 μl of autoclaved water supplemented with ampicillin (targeting Gram-negative bacteria; 1 mg ml^{-1}), kanamycin (Gram-positive and Gram-negative bacteria; 1 mg ml^{-1}), polymyxin B (Gram-negative bacteria; 1 mg ml^{-1}), neomycin (yeast; 1 mg ml^{-1}) and vancomycin (Gram-positive bacteria; 0.5 mg ml^{-1}). The force-feeding was done by filling the 10 ul Hamilton syringe (needle size 26 ga, needle L 51 mm, Sigma-Aldrich, UK) with 10 μL of antibiotic and then removing the bubble. The mouth of the insect was inserted into the syringe with the needle fixed, and manually supplied with 10 μL of solution (Ramarao et al., 2012). Controls without antibiotics were also included. Cultured bacterial contamination was confirmed using tryptic soy agar (TSA) and yeast extract-peptone-dextrose (YPD) medium at 24 h after antibiotic treatment. To confirm bacterial contamination by culture-independent methods, the 16S rRNA gene was amplified by PCR using Taq DNA polymerase with primers 27F (5′-AGAGTTTGATCCTGGCTCAG-3′) and 1492R (5′-GGTTACCTTGTTACGACTT −3′). Yeast contamination was assessed by amplifying 26S rDNA using primers NL-1 (5′-GCATATCAATAAGCGGAGGAAAAG-3′) and NL-2 (5′-GGTCCGTGTTCAAGACGG-3′). Fungal contamination was assessed by amplifying ITS region using primers ITS1 (5′-TCCGTAGGTGAACCTGCGG-3′) and ITS4 (5′-TCCTCCGCTTATTGATATGC-3′).

Measuring larval weight following feeding on beeswax, PE or an artificial diet

To investigate the possible degradation of beeswax and PE as an energy source, the weight and survival rate of larvae fed on beeswax, PE or an artificial diet were measured using second instar larvae (starved larvae were included as controls). Low density PE was purchased from Thermo-Fisher Scientific, USA (Cat# B1180, powder type, 500 micron). The 100 mg food source and one larva per well were placed. For the combination treatment of beeswax and nutrition-rich food, 100 mg single and combination treatments after mixing according to each ratio were subdivided. At three days after application of food treatment, the consumed food by larva was estimated by detection of left-over food. (Figure S1). Experiments were carried out by starving larvae for 3 days followed by each food (beeswax or PE; artificial food; 1: 9; 5: 5, 9: 1 ratio) feeding at a rate of 100 mg per larvae. Weight and survival rate were determined for 15 days, 20 larvae were included per treatment and all experiments were repeated in triplicate.

Honey and wax diets

The wax diet consisted of a 9:1 ratio of beeswax and artificial diet, and last instar larvae were fed a nutrition-rich diet or a nutrition-rich diet with beeswax prior to metatranscriptome analysis. For GC-MS and growth analyses, early larvae were fed an artificial diet or beeswax alone (negative controls were starved). After 1 day, *G. mellonella* individuals were collected for further processing.

GC-MS quantification of fatty acids

For analysis of beeswax degradation products in the *G. mellonella* gut, beeswax alone was fed for 12 h and gut samples were harvested (five replicates were included). Starvation conditions were employed in controls. To confirm the degradation products in the presence or absence of intestinal microorganisms, the antibiotic mix was administered as described above and beeswax was fed for 12 h. Lipids were then extracted from *G. mellonella* gut samples using 1 mL of chloroform:methanol (2:1) per larva. The solvent was evaporated using Scan Vac Scanspeed vacuum centrifuge 40 (LaboGene, S. Korea). The extract was reconstituted in 100% hexane for GC-MS quantification of total fatty acids, total hydrocarbons and profiling of long-chain fatty acids. For each condition, five animals were used, and experiments were carried out using a 5975C gas chromatograph (Agilent) equipped with an HP-5MS column

(30 m × 0.25 mm internal diameter, 0.25 μm width; Agilent) with helium as a carrier gas and injection of 1 μL of each sample. The initial oven temperature was set to 70°C, increased to 230°C at 10°C per min, and held for 2 min at this temperature.

DNA isolation

A single larva was ground using a pestle in a 1.5 mL microcentrifuge tube with 400 μL of DNA extraction buffer consisting of 10 mM Tris-HCl pH 8.0, 0.2 M EDTA pH 8.0, 20 μg/ml RNase, 0.5% sodium dodecyl sulfate (SDS) and 10 μL of 100 μg/ml proteinase K (Kambhampati and Rai, 1991). The sample was vortexed and incubated at 56°C to lyse insect tissues completely over a 1−3 h period. After incubation, the lysate appeared viscous, and 400 μL of phenol:chloroform:isoamylalcohol (25:24:1, pH 8.0) was added and vortexed to homogeneity, resulting in a layer of white precipitate. After vortexing vigorously for 20 s, samples were centrifuged at 13−16,000 × g for 20 min, resulting in a tight pellet. Samples not containing a tight pellet were incubated on ice for 5 min, and centrifugation was repeated until a tight pellet was obtained. A 350 μl aliquot of the supernatant was transferred to a new 1.5 mL microcentrifuge tube, and the phenol:chloroform:isoamylalcohol extraction step was repeated. After centrifugation, 300 μl of the supernatant was transferred to a new 1.5 mL microcentrifuge tube and 300 μl of chloroform:isoamyl alcohol (24:1) solution was added. After vortexing vigorously for 20 s and centrifugation at 13,000−16,000 × g for 20 min, 250 μl of the supernatant was transferred to a new 1.5 mL microcentrifuge tube and 250 μl of isopropanol was added and incubated at −20°C for 20 min. After centrifugation at 13,000−16,000 × g for 20 min, the supernatant was removed and 1 mL of 70% EtOH was added. After centrifugation at 13−16,000 × g for 5 min, the supernatant was removed and dried. DNA was then dissolved in 8 mM NaOH.

Estimation of G. mellonella genome size

To investigate the genome of *G. mellonella*, we constructed a library with an insert size of 400 bp according to the Illumina sequencing manufacturer's protocol and performed sequencing using an Illumina HiSeq platform. Low-quality sequencing data were removed by applying filtering criteria (PCR duplicated, adaptor contaminated and < Q20 quality) to reduce the effects of sequencing errors in the *K*-mer analysis. After filtering, 5′ and 3′ low-quality short sequencing data were trimmed using an in-house script. *K*-mer analysis was performed using final short sequencing data, and the genome size was estimated before genome assembly based on the *K*-mer spectrum as previously described (Li et al., 2010). If the *K*-mer frequency obeys a Poisson distribution, when the coverage is sufficient, the genome size can be estimated using the following expression:

Predicted genome size = Total sequenced bases / Depth = Total *K-mer number* / *K-mer frequency*

PacBio data generation

Wax moth genomic DNA was extracted from a single 4th stage larva, which is the longest period. Because PacBio RS II sequencing requires more genomic DNA than the Illumina method, we used a single wax moth larva to reduce the heterogeneity among individuals. Large insert PacBio library preparation was performed according to the Pacific Biosciences MagBeadOneCellPerWell protocol (https://www.pacb.com/wp-content/uploads/2015/09/Procedure-Checklist-Preparing-MagBeads-for-Sequencing.pdf). We generated long-read data using a PacBio RS II instrument and P6C4 sequencing chemistry. As a result, we used 32 single-molecule real-time (SMRT) cells and obtained 65-fold redundant whole genome sequencing data.

Genome assembly

Sequenced reads were assembled using Falcon Assembler v0.3.0 (Chin et al., 2013) with a length_cutoff parameter of 12 kb and a length_cutoff_pr of 12 kb. The detailed Falcon Assembler config options were following. Assembly was performed with error correction using Illumina HiSeq data. First, Illumina HiSeq data were mapped to assembled data using BWA-MEM (Li and Durbin, 2009) with default options, and Indel re-alignment and base recalibration were performed using Sentieon (Freed et al., 2017) with default options. Variants (SNVs and INDELs) were called using Sentieon Haplotyper. Error correction was performed by replacing homo variants in the variant call format (*vcf.*) file. We conducted error correction five times in succession due to numerous complex indels using an in-house script.

```
input_type = raw
# The length cutoff used for seed reads used for initial mapping
length_cutoff = 12000
# The length cutoff used for seed reads usef for pre-assembly
length_cutoff_pr = 12000
sge_option_da = -pe smp 3 -q bigmem
sge_option_la = -pe smp 3 -q bigmem
sge_option_pda = -pe smp 3 -q bigmem
sge_option_pla = -pe smp 3 -q bigmem
sge_option_fc = -pe smp 3 -q bigmem
sge_option_cns = -pe smp 3 -q bigmem
pa_concurrent_jobs = 10
ovlp_concurrent_jobs = 10
```

pa_HPCdaligner_option = -v -dal4 -t16 -e.70 -l500 -s500
ovlp_HPCdaligner_option = -v -dal4 -t32 -h60 -e.96 -l500 -s500
pa_DBsplit_option = -x500 -s50
ovlp_DBsplit_option = -x500 -s50
falcon_sense_option = –output_multi–min_idt 0.70–min_cov 4–local_match_count_threshold 2–max_n_read 200–n_core 2
overlap_filtering_setting = –max_diff 100–max_cov 150–min_cov 10–bestn 10

Gene prediction and integration of gene sets

We proceeded with a homology gene prediction, an *ab initio* gene prediction and a transcript-based gene prediction, and then integrated the resulting gene sets using EVidenceModeler. The homology gene prediction was performed using Exonerate software v2.2.0 (Slater and Birney, 2005) with protein sequences from *Drosophila melanogaster*, *Papilioxuthus*, *Bombyx mori* and *Plutella xylostella*. The transcript-based prediction was performed using the TopHat2 (Kim et al., 2013) and Cufflinks (Roberts et al., 2011) pipelines, and the Program to Assemble Spliced Alignment (PASA) (Li et al., 2010) pipeline. All 11 samples (6 fat body samples of nutrition-enrich fed and beeswax fed larvae; 2 gut samples of nutrition-enrich fed larvae and 3 gut samples of beeswax fed larvae) were mapped to the assembly using TopHat2 v2.0.9, and gene sets were generated using Cufflinks v2.1.1 with default settings. All 11 samples were also merged, and transcriptome data from three methods (*de novo* assembly by Trinity v2.3.0 (Grabherr et al., 2011), reference-based assembly by TopHat2 and Cufflinks, and reference-guided assembly by Trinity) were integrated using PASA v2.0.2. The *ab initio* gene prediction was performed using AUGUSTUS v3.0.3 (Stanke et al., 2006), Maker v2.31.9 (Cantarel et al., 2008), SNAP v2013-11-29 (Korf, 2004), GlimmerHMM v3.0.4 (Majoros et al., 2004), Genemark v4.32 (Besemer and Borodovsky, 2005) and GeneID v1.4 (Parra et al., 2000). Finally, the prediction results of four homology gene prediction sets, 24 transcript-based gene prediction sets and six *ab initio* prediction sets were integrated using Evidence modeler.

Repeat annotation

We searched the tandem repeat region of the *G. mellonella* genome using Tandem Repeats Finder v4.07b (Benson, 1999). We also identified TEs through homology-based approaches employed using Repbase v19.03 (Jurka et al., 2005), a widely used database of known repeats, and a *de novo* repeat library generated by RepeatModeler v1.0.7 (Price et al., 2005). This database was used to identify repetitive regions with software programs such as RepeatMasker v4.0.5 and RMBlast v2.2.28. The predicted repetitive elements were merged for statistical analysis using in-house scripts.

Assembly and gene set assessment

The completeness of coding regions in the *G. mellonella* genome was evaluated using assembled RNA-seq transcripts from three larva fat body transcriptome datasets and the Trinity program (Grabherr et al., 2011) with default options, and mapped to the *G. mellonella* genome assembly using Blat (Kent, 2002) with default options. Coverage of transcripts on the scaffold was calculated using an in-house script. Also, the quality of the assembly and protein-coding gene sets was assessed using BUSCO software (Simão et al., 2015).

Annotation of protein-coding genes

The final gene set was subjected to gene function and pathway, domain and GO annotation. Gene functions were annotated based on the best match in the alignment using BLASTp with SwissProt, TrEMBL and FlyBase databases (UniProt Consortium, 2012; Bairoch and Apweiler, 2000; St Pierre et al., 2014) with an alignment criterion e-value < 10^{-5}. Gene domains and motifs were searched using InterProScan v5.13 (Zdobnov and Apweiler, 2001) with public protein databases Pfam (Punta et al., 2012), SMART (Ponting et al., 1999), PATHER (Mi et al., 2005), ProDom (Bru et al., 2005), PRINT (Attwood and Beck, 1994) and PROSITE (Hulo et al., 2006). GO accessions for each gene were assigned from the corresponding InterPro entries. Pathways were determined using the KEGG Automatic Annotation Server (KAAS) web program (Moriya et al., 2007).

Orthologous gene clustering

Orthologous gene families were constructed for evolutionary analyses using OrthoMCL v2.0.9 (Li et al., 2003) using 13 insect genomes and one Arachnida outgroup (*Acyrthosiphon pisum*, *Amyelois transitella*, *Anopheles gambiae*, *Apis mellifera*, *Bombyx mori*, *Drosophila melanogaster*, *Harpegnathos saltator*, *Galleria mellonella*, *Nasonia vitripennis*, *Papilio xuthus*, *Pediculus humanus*, *Plutella xylostella*, *Tetranychus urticae* and *Tribolium castaneum*). Protein sequences from all species were clustered using BLASTp with the criterion e-value < 10^{-5}. All genomes and gene sets for species other than *G. mellonella* were downloaded from the NCBI database.

Phylogenetic analysis

To construct a phylogenetic tree, we used the MUSCLE (Edgar, 2004) alignment program for single-copy gene family protein sequences, and filtered the low-quality alignment using the trimAl (Capella-Gutiérrez et al., 2009) program with the 'gappyout' option. The phylogenetic tree was constructed using RAxM (Stamatakis, 2014) software with the PROTGAMMAJTT model and 100 bootstrap replicates. To estimate the divergence times, we used the MEGA7 (Kumar et al., 2016) program with the filtered protein sequences. We then used the CODEML program in the PAML 4.5 package (Yang, 2007) for evolutionary analysis. The one-ratio model, which allows only a single dN/dS ratio for all branches, was used to estimate the general selective pressure acting among

all species. A free-ratios model was used to analyze the dN/dS ratio along each branch. To further examine potential positive selection, the branch-site test of positive selection was conducted (Zhang et al., 2005).

Gene expansion/contraction

We performed gene expansion/contraction analysis using CAFÉ software v3.1 (Han et al., 2013) with the estimated phylogenetic tree information at $p < 0.05$ indicating significantly altered gene families. The multiple sequence alignments and phylogenetic analysis were conducted with expanded gene families in *G.mellonella* using ClustalW2 program (Larkin et al., 2007)

RNA isolation

Total RNA was isolated from a single larval tissue using TRIzol reagent (Invitrogen). After grinding a single larva with TRIzol reagent using a pestle in a 1.5 mL micro-centrifuge tube, RNA was phase separated using chloroform, precipitated with an equal volume of isopropanol and washed with 75% ethanol following the manufacturer's instructions. Total RNA was suspended in 50 μL of 0.1% v/v diethylpyrocarbonate (DEPC)-treated water and stored at −80°C. Total RNAs of 11 samples were sequenced using Illumina HiSeq platforms according to the manufacturer's instructions

Analysis of DEGs

We proceeded with reference indexing using Bowtie2 to map the 11 RNA-seq samples to the *G. mellonella* assembly. After indexing, raw data were mapped to the assembly using TopHat2 with default settings. Expression values from the mapped BAM files were calculated using Cufflinks. To reduce bias between samples, expression values were normalized using the 3rd upper quantile normalization method. When calculating DEGs, fat body samples were compared with each other, as were gut samples. The t test was performed using the Welch's t test method, and DEGs were selected when the FDR was < 0.05. The Welch's t test was applied using the following formula:

$$t = \frac{\overline{X}_1 - \overline{X}_2}{\sqrt{\frac{s_1^2}{N_1} + \frac{s_2^2}{N_2}}}$$

Where X, s, and N are the samples mean, the unbiased sample standard deviation and sample size for the group.

Measuring the GC content of the G. mellonella genome

The GC content of the *G. mellonella* genome was estimated using a sliding window approach. Briefly, a 500 bp (250 bp stepwise) sliding window was employed to scan along the genome and calculate the GC content. We found that the average GC content was ~33.8%, which is within the range of other Lepidoptera.

tRNA annotation

The tRNA of 26 Insecta and 2 Arachnida that included 14 species of Lepidoptera and 6 species of Dipteran were calculated using tRNA-scan. As a result, 14 species of Lepidoptera and Aranea were expanded the Ala-tRNA (Lepidoptera and Aranea mean: 49.93333, Other mean: 27, $p = 1.2 \times 10^{-2}$), Gly-tRNA (Lepidoptera and Aranea mean: 43.71429, Other mean: 19.76923, P value: $p = 2.4 \times 10^{-5}$) compared with the other insects and *T. urticae.* Ala and Gly are the main amino acids that make up Silk (Chevallier and Garel,1982; Xia et al., 2004).

Metatranscriptomics

RNA-seq data were generated using a TruSeq Stranded Total RNA kit to obtain intestinal microbial RNA data from the *G. mellonella* intestine. Since RNA-seq data were from a mixture of *G. mellonella* intestinal tissue and intestinal microbes, we used the unmapped bam file by mapping the raw data to TopHat2 in the *G. mellonella* assembly. We also filtered out reads for which read pairs were mapped to the reference using an in-house Perl script. Putative RNA reads of microbiome origin were assembled by Trinity using the paired-end mode.

QUANTIFICATION AND STATISTICAL ANALYSIS

Statistical significances are reported in the Figures and Figure Legends. Data is considered to be statistically significant when $p < 0.05$ by two way ANOVAs test and two-tailed Student's t test. In figures, asterisks denote statistical significance as calculated by Student's t test (*, $p < 0.05$; **, $p < 0.01$; ***, $p < 0.001$; ****, $p < 0.0001$). Statistical analysis was performed in R program (R Development core team 2011).

DATA AND SOFTWARE AVAILABILITY

The *Galleria mellonella* genome have been deposited in the NCBI under ID codes SUB2718188 and RNA sequence data have been deposited in the NCBI under ID codes PRJNA386430, SAMN07108742 - SAMN07108763.